# Carbon-Aware Intrusion Detection: A Comparative Study of Supervised and Unsupervised DRL for Sustainable IoT Edge Gateways

Saeid Jamshidi\*, Foutse Khomh, Kawser Wazed Nafi, Amin Nikanjam, Samira Keivanpour, Rolando Herrero, Omar Abdul-Wahab, and Martine Bellaiche

Abstract—The rapid expansion of the Internet of Things (IoT) has intensified cybersecurity challenges, particularly in mitigating Distributed Denial-of-Service (DDoS) attacks at the network edge. Traditional Intrusion Detection Systems (IDSs) face significant limitations, including poor adaptability to evolving and zero-day attacks, reliance on static signatures and labeled datasets, and inefficiency on resource-constrained edge gateways. Moreover, most existing DRL-based IDS studies overlook sustainability factors such as energy efficiency and carbon impact. To address these challenges, this paper proposes two novel Deep Reinforcement Learning (DRL)-based IDS: DeepEdgeIDS, an unsupervised Autoencoder-DRL hybrid, and AutoDRL-IDS, a supervised LSTM-DRL model. Both DRL-based IDS are validated through theoretical analysis and experimental evaluation on edge gateways. Results demonstrate that AutoDRL-IDS achieves 94% detection accuracy using labeled data, while DeepEdgeIDS attains 98% accuracy and adaptability without labels. Distinctly, this study introduces a carbon-aware, multiobjective reward function optimized for sustainable and real-time IDS operations in dynamic IoT networks.

Index Terms—Intrusion Detection System, Deep Reinforcement Learning, Autoencoders, LSTM, IoT, Edge Computing, Carbon Awareness, and Resource Efficiency.

# I. INTRODUCTION

The Internet of Things (IoT) has rapidly evolved into a ubiquitous paradigm, interconnecting billions of devices across various domains, including healthcare, smart cities, and industrial automation [1], [2]. However, this rapid expansion has also introduced significant cybersecurity challenges due to the decentralized nature, constrained resources, and dynamic topologies of IoT systems [3], [4]. Among these, Distributed Denial-of-Service (DDoS) attacks remain one of the most severe threats, capable of overwhelming resource-limited devices and disrupting critical services [5], [6].

Traditional Intrusion Detection Systems (IDSs) struggle to de-

Saeid Jamshidi\*, Kawser Wazed Nafi, and Foutse Khomh are with the SWAT Laboratory, Polytechnique Montréal, Québec, Canada, H3T 1J4.

Amin Nikanjam is with the Huawei Distributed Scheduling and Data Engine Lab (work conducted while at Polytechnique Montréal).

Rolando Herrero is with the College of Engineering, Northeastern University, Boston, MA, USA.

Samira Keivanpour is also affiliated with Poly Circle X.O, Polytechnique Montréal, Québec, Canada, H3T 1J4.

Omar Abdul-Wahab and Martine Bellaiche are with the Department of Computer and Software Engineering, Polytechnique Montréal, Québec, Canada, H3T 1J4.

\*Corresponding author: saeid.jamshidi@polymtl.ca

tect zero-day attacks<sup>1</sup>, where previously unseen threats evade predefined attack signatures [7]. Given limited computational resources and the absence of robust security mechanisms, IoT gateways face a high risk of compromise, underscoring the need for proactive and resilient edge defense mechanisms [8], [9]. Conventional IDS solutions, including signature-based and anomaly-based models, remain inadequate for the dynamic and heterogeneous nature of IoT traffic [10], [11], [12]. Signature-based IDSs rely on static rules and often fail to detect emerging and adversarial attack patterns. In contrast, anomaly-based IDSs, although capable of identifying unknown threats, frequently yield high false positive rates, which limits their feasibility for real-time deployment. Consequently, there is a growing demand for adaptive and intelligent detection mechanisms that can learn and evolve in response to real-time IoT traffic dynamics.

Deep Reinforcement Learning (DRL) has emerged as a promising paradigm for smart IDS [13], [14], [15]. In contrast to static approaches, DRL-based IDSs continuously interact with the environment, autonomously learning to detect complex and evolving attack behaviors. Nevertheless, deploying DRL-based IDSs in real-world IoT networks presents unique challenges. IoT edge gateways are resource-constrained in terms of processing, memory, and energy capacity, creating a fundamental trade-off between detection accuracy, adaptability, and resource efficiency [16]. Moreover, the choice of learning paradigm—supervised versus unsupervised—critically affects performance in dynamic network conditions [17], [18], [19], [20], [21]. Supervised learning benefits from labeled data to improve accuracy but struggles to adapt to zeroday threats, whereas unsupervised learning excels in detecting novel behaviors but may suffer from higher false alarm rates if not well-tuned[22]. These limitations underscore a critical research gap: existing DRL-based IDS rarely address the dual challenge of adaptability and sustainability. Most previous studies [23][24][25][26] focus primarily on detection accuracy while overlooking the energy and carbon footprint of Deep Learning (DL) operations, an increasingly important concern in large-scale IoT deployments.

To address these challenges, this paper proposes two novel DRL-based IDS solutions for DDoS detection at the edge gateway, namely DeepEdgeIDS and AutoDRL-IDS. To the

<sup>1</sup>Zero-day attacks exploit vulnerabilities unknown to vendors and the public, bypassing traditional signature-based systems such as Snort.

best of our knowledge, no previous work has combined their respective learning paradigms with customized state, action, and reward formulations alongside closed-loop mitigation on real-world, resource-limited edge gateways. DeepEdgeIDS employs an unsupervised approach, integrating Autoencoders (AE) with DRL to autonomously learn latent representations of benign traffic and detect anomalies without labeled data. This makes it particularly effective in dynamic IoT networks where labeled datasets are scarce. In contrast, AutoDRL-IDS adopts a supervised LSTM-DRL structure that leverages labeled data to optimize detection policies and improve precision in structured attack scenarios. Both models are deployed and evaluated on physical edge gateways to assess their real-world feasibility and scalability. Our analysis compares the two novel solutions in terms of detection accuracy, adaptability, resource efficiency, and environmental sustainability. Beyond conventional performance metrics, this study explicitly introduces a carbonaware optimization objective within the DRL reward functionan aspect largely ignored in existing IDS literature. The reward formulation jointly optimizes detection rate, latency, memory usage, and estimated carbon footprint, enabling balanced, sustainable decision-making on edge devices. Additionally, a mathematical model links memory and energy consumption to carbon emissions as continuous feedback signals within the learning process. Theoretical convergence of DeepEdgeIDS is proven via the Bellman contraction [27] property under bounded rewards, ensuring stable policy learning in dynamic traffic conditions. Furthermore, to validate the experimental findings, Analysis of Variance (ANOVA) [28] is employed to statistically assess performance differences between the proposed models across multiple metrics, including detection probability, response time, latency, CPU usage, and energy efficiency. The findings demonstrate that DeepEdgeIDS outperforms AutoDRL-IDS in detection accuracy, response time, and adaptability to zero-day attacks, while consuming less CPU power and exhibiting faster convergence. In contrast, AutoDRL-IDS achieves more consistent performance in structured attack scenarios and demonstrates slightly higher energy efficiency under low-traffic conditions. The main contributions are summarized as follows:

- Design of Two Adaptive and Sustainable DRL-Based IDS for Edge Gateways: This paper introduces two novel DRL-based IDS: AutoDRL-IDS, a supervised LSTM-DRL model that leverages labeled data to optimize detection accuracy, and DeepEdgeIDS, an unsupervised AE-DRL hybrid capable of autonomously detecting anomalies without labels. Both DRL-based IDS are explicitly designed for energy-efficient and sustainable operation at the edge gateways.
- Comparative Evaluation of Supervised and Unsupervised DRL Paradigms: A comparison is conducted between supervised and unsupervised DRL-based IDS approaches, examining their trade-offs in detection accuracy, adaptability to zero-day attacks, false positive rates, computational efficiency, and environmental sustainability across dynamic IoT scenarios.
- Real-World Implementation and Carbon-Aware Per-

formance Assessment: Both DRL-based IDS are deployed on physical edge gateways under live DDoS attack. Their performance is evaluated across critical dimensions, including detection accuracy, response time, CPU and memory usage, energy efficiency, and estimated carbon emissions, establishing the first carbonaware benchmarking of DRL-based IDS systems at the edge.

Carbon-Aware Mathematical Modeling and Theoretical Validation: A novel quantitative model is proposed that integrates energy consumption, memory usage, and carbon emissions as continuous feedback variables within the DRL reward function, enabling sustainability-aware decision-making. Furthermore, the convergence of DRL-based IDS is theoretically proven via the Bellman contraction property under bounded rewards, ensuring stable learning in dynamic IoT networks.

The remainder of this paper is organized as follows. Section II reviews related IDS research. Sections III describe the proposed solutions. Section IV outlines the experimental setup and dataset. Section V presents evaluation results, while Section VIII discusses key understanding. Section VIII outlines limitations and future work, and Section IX concludes the paper.

#### II. RELATED WORK

This section provides an overview of existing IDS solutions in IoT networks, highlighting advancements in ML and DRL techniques for real-time threat detection and mitigation.

## A. ML-Based IDS for DDoS Detection

Several studies have proposed intelligent ML-based frameworks to enhance DDoS detection in IoT networks. Yousuf et al. [29] introduced DALCNN, an RNN-based model integrated into an SDN framework, achieving 99.98% accuracy with enhanced detection capabilities and minimal false positives. Pandey et al. [30] explored entropy-based methods, demonstrating that  $\phi$ -entropy with quartile-based thresholds improves detection precision but requires further enhancement in recall. Ahmad et al. [31] proposed a big data-driven ensemble model combining SVM, CNN, and GRU, optimized using the Slime Mould Algorithm (SMA), achieving 98.45% accuracy while reducing false positives and improving detection speed. Nguyen et al. [32] developed a hybrid learning model combining SOCNN, LOF, and iNNE, demonstrating superior detection of unknown and adversarial attacks across benchmark datasets. Gupta et al. [33] introduced a lightweight CNN-based framework for resource-constrained IoT devices, achieving 99.38%, accuracy and outperforming conventional ML classifiers. These works collectively highlight the effectiveness of ML-based IDS in addressing evolving DDoS threats while showcasing the need for further innovation in reducing computational overhead and enhancing adaptive capabilities.

#### B. DRL-Based IDS for DDoS Detection

DDoS attacks in IoT remain challenging due to the limited computational resources of edge devices and the dynamic nature of threats. DRL has emerged as a promising paradigm, enabling IDS to learn and adapt to cyber threats autonomously. Feng et al. [23] introduced a Soft Actor-Critic (SAC)-based DRL approach that utilizes lightweight unsupervised classifiers at edge gateways to detect volumetric and stealthy low-rate DDoS attacks, achieving 91% accuracy while maintaining low resource overhead. Liu et al. [34] proposed a hierarchical DRL framework that mitigates multi-layer DDoS attacks, achieving 97%, detection accuracy by leveraging cross-layer threat intelligence. Vadigi et al. [35] integrated federated learning with DRL to enhance scalability and privacy in IoT security, achieving 96.7% accuracy on the NSL-KDD dataset and 99.66% on the ISOT-CID dataset. Their dynamic attention mechanism enables real-time adaptation to evolving attack patterns without sharing raw data, preserving data privacy in decentralized environments. Beyond DDoS detection, RL has been effectively employed in broader IDS scenarios. Ramana et al. [36] implemented a DQN-based IDS capable of detecting both binary and multiclass attacks in IoT networks, demonstrating high scalability and accuracy across the UNSW-NB-15 and CICIDS2017 datasets. Ma et al. [37] proposed a Minimax-DQN model that leverages game-theoretic principles to optimize intrusion response strategies in fog computing environments, thereby improving response time and attack mitigation efficiency. Zhang et al. [38] introduced a zero-sum game-theoretic DRL model to secure IoT edge devices against adversarial behaviors, ensuring robust threat detection with minimal computational footprint.

DRL techniques have also demonstrated effectiveness in malware and botnet detection, which is crucial for securing IoT networks. Al-Garadi et al. [39] developed a DRL-driven botnet detection framework that achieves over 99%, detection accuracy across different lifecycle stages of malware, addressing challenges such as model drift and evolving attack patterns. Their work underscores the potential of DRL in proactive and adaptive IoT security solutions.

The literature on IDS for IoT has shown progress in ML and DRL-based models for DDoS detection, enhancing both accuracy and adaptability. However, major challenges persist in detecting zero-day attacks, ensuring computational efficiency, and enabling real-time deployment on resource-constrained edge gateways. To address these gaps, this work introduces two novel DRL-based IDS solutions: DeepEdgeIDS, an unsupervised AE-DRL hybrid, and AutoDRL-IDS, a supervised LSTM-DRL model, both of which are implemented and evaluated in real-time on edge gateways. Distinct from existing studies, the proposed systems integrate a carbonaware optimization objective within the DRL reward function. jointly improving detection accuracy, resource utilization, and environmental sustainability. This comparative analysis of supervised and unsupervised paradigms under realistic IoT conditions offers a new understanding of achieving scalable, efficient, and sustainable intrusion detection.

#### III. PROPOSED SOLUTIONS

This section introduces two proposed DRL-based IDSs, namely DeepEdgeIDS and AutoDRL-IDS.

#### A. DeepEdgeIDS

DeepEdgeIDS is a DRL-based IDS designed to detect and mitigate DDoS attacks at the edge gateways. The DRL-based IDS integrates an AE-based unsupervised feature extractor with a Deep Q-Network (DQN) for adaptive mitigation. Moreover, by combining self-learned representations with reinforcement-driven control, DeepEdgeIDS enables real-time adaptability, energy efficiency, and carbon-aware sustainability in dynamic IoT networks. As illustrated in the Figure. 1, DeepEdgeIDS combines AE-based feature extraction with DRL-based decision making. Network traffic is continuously monitored and encoded into latent features, with reconstruction error used to detect anomalies. Deviations are forwarded to the DQN agent, along with raw traffic statistics, where the agent assesses the severity and selects the optimal mitigation actions. Experience replay ensures stable learning, while a sustainability-driven reward balances detection, latency, energy, and carbon cost.

1) AE-Based Feature Extraction: The AE learns a compressed representation of normal traffic patterns and identifies anomalies via reconstruction error. Given input features  $x_t$ :

$$h_t = f_{\theta}^{encoder}(x_t), \quad \hat{x}_t = f_{\theta}^{decoder}(h_t),$$
 (1)

The reconstruction error is:

$$A_s = \|x_t - \hat{x}_t\|^2, \tag{2}$$

where large  $A_s$  indicates abnormal activity. Traffic is flagged if

$$A_s > \tau_A \Rightarrow \text{DDoS suspected.}$$
 (3)

These AE-derived features augment the DQN state for adaptive learning.

2) Mitigation Strategy and State Modeling: The detection-mitigation process is modeled as a Markov decision process with state:

$$s_t = \{P_{rate}, SYN_{count}, ACK_{count}, A_s, h_t\},$$
(4)

and action space:

$$A = \{a_1, a_2, a_3, a_4\}. \tag{5}$$

Q-values are updated using:

$$Q(s_t, a_t) = R(s_t, a_t) + \gamma \max_{a'} Q(s_{t+1}, a'),$$
 (6)

ensuring long-term optimization. To formalize this in controltheoretic form, the mitigation dynamics can be expressed as:

$$\dot{x}(t) = f(x(t)) + g(x(t))u(t),$$
 (7)

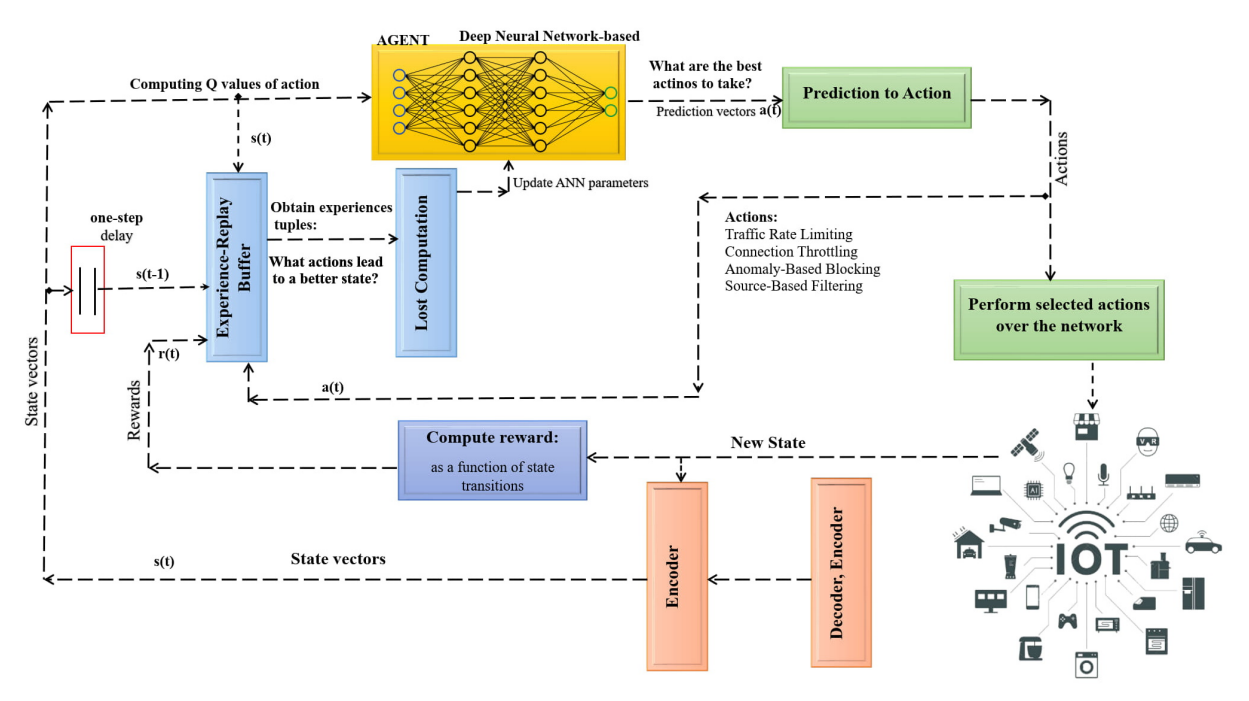


Fig. 1: Overview of the proposed DeepEdgeIDS architecture for DDoS detection.

where x(t) is the network state vector, and  $u(t) \in A$  is the mitigation control input. The optimal policy  $\pi^*$  minimizing cumulative cost:

$$J(\pi) = \int_0^T \left( \mathcal{L}(x(t), u(t)) + \zeta C_{emission}(t) \right) dt, \qquad (8)$$

subject to energy constraints  $E_{overhead}(t) \leq E_{max}$ , satisfies the Hamilton–Jacobi–Bellman (HJB) [40] equation:

$$0 = \min_{u \in A} \left\{ \mathcal{L}(x, u) + \nabla_x V(x)^\top (f(x) + g(x)u) \right\}, \quad (9)$$

where V(x) is the value function approximated by the DQN,  $V(x) \approx Q(s,a)$ .

3) Sustainability-Aware Reward Function: Each action is evaluated through a multi-objective reward combining accuracy, delay, and environmental efficiency:

$$R(s_t, a_t) = \alpha DR - \beta FPR - \lambda_L L_{resp} - \delta E_{overhead} - \epsilon M_{util} - \zeta C_{emission}, \quad (10)$$

where DR and FPR denote detection and false-positive rates. To ensure stability under constrained energy budgets, a Lyapunov function is introduced:

$$V_t = \frac{1}{2} \|Q_t - Q^*\|^2.$$
 (11)

Differentiating along the training trajectory yields:

$$\dot{V}_t = (Q_t - Q^*)^\top (\dot{Q}_t - \dot{Q}^*) \le -\eta \|Q_t - Q^*\|^2,$$
 (12)

which ensures exponential convergence to the optimal policy when  $\eta > 0$ .

4) Modeling Energy, Memory, and Carbon Cost: Sustainability terms are modeled as:

$$E_{overhead}(t) = \int_{0}^{\Delta t} P(\tau) d\tau = P_t \cdot \Delta t, \tag{13}$$

$$M_{util}(t) = \frac{M_{active}(t)}{M_{total}},$$
(14)

$$C_{emission}(t) = \int_{0}^{\Delta t} \kappa(\tau) P(\tau) d\tau \approx E_{overhead}(t) \kappa_{t}, \quad (15)$$

and boundedness is guaranteed since:

$$E_{overhead}(t) \le P_{max} \Delta t, \quad C_{emission}(t) \le \kappa_{max} E_{overhead}(t).$$
(16)

The optimal steady-state sustainability point occurs when:

$$\frac{\partial R}{\partial E_{overhead}} + \zeta \kappa_t = 0 \Rightarrow E_{opt} = -\frac{\zeta \kappa_t}{\partial R/\partial E_{overhead}}.$$
 (17)

5) Experience Replay and Convergence: The Bellman [41] operator  $\mathcal{T}$  satisfies:

$$\|\mathcal{T}Q_1 - \mathcal{T}Q_2\|_{\infty} \le \gamma \|Q_1 - Q_2\|_{\infty},$$
 (18)

guaranteeing convergence to  $Q^*$ . Using stochastic approximation, the update:

$$Q_{k+1}(s, a) = (1 - \eta_k)Q_k(s, a) + \eta_k \left[ R_t + \gamma \max_{a'} Q_k(s', a') \right],$$
(19)

converges a.s. if  $\sum_k \eta_k = \infty$ ,  $\sum_k \eta_k^2 < \infty$ .

6) Control-Theoretic Stability Analysis: Let the overall closed-loop dynamics be:

$$x_{t+1} = f(x_t) + g(x_t)\pi_{\theta}(s_t),$$
 (20)

and define a Lyapunov [42] function  $V(x_t) = x_t^{\top} P x_t$  with  $P = P^{\top} > 0$ . Stability holds if:

$$\Delta V = V(x_{t+1}) - V(x_t) \le -x_t^{\top} Q x_t - \pi_{\theta}(s_t)^{\top} R \pi_{\theta}(s_t),$$
(21)

for some positive definite matrices Q,R. Therefore, the learned policy  $\pi_{\theta}$  is asymptotically stable under bounded power and carbon constraints.

7) Adaptive Source Filtering: Persistent threats are identified using:

$$P_{attack}(i) = \frac{1}{T} \sum_{t=1}^{T} \mathbb{1} \left( A_s(i,t) > \tau_A \right), \tag{22}$$

and IPs with  $P_{attack}(i) > \tau_P$  are blacklisted for long-term prevention.

8) DeepEdgeIDS Pipeline: Algorithm1 represents the closed-loop control of DeepEdgeIDS, integrating AE-based anomaly extraction with a DQN for adaptive mitigation. At each timestep t, network traffic  $x_t$  is encoded as  $h_t = f_{\theta}^{encoder}(x_t)$ , and the reconstruction error  $a_s = \|x_t - \hat{x}_t\|^2$  quantifies anomaly deviation. If  $a_s > \tau_A$ , the state  $s_t = \{P_{rate}, SYN_{count}, ACK_{count}, a_s, h_t\}$  is formed and the optimal mitigation  $a_t = \arg\max_a Q(s_t, a)$  is chosen. Each action is mapped to a predefined policy, including rate limiting, throttling, blocking, and source filtering. The reward is multiobjective:

$$r_t = \alpha DR_t - \beta FPR_t - \lambda_L L_t - \delta E_t - \epsilon M_t - \zeta C_t,$$

balancing detection accuracy, latency, and sustainability. Qvalues are iteratively updated as

$$Q_{new}(s_t, a_t) = (1 - \eta)Q(s_t, a_t) + \eta[r_t + \gamma \max_{a'} Q(s_{t+1}, a')],$$

with gradients  $\nabla_{\theta_Q}(Q(s_t,a_t)-y_t)^2$  driving convergence toward  $Q^*$ . The Bellman operator  $\mathcal{T}$  satisfies  $\|\mathcal{T}Q_1-\mathcal{T}Q_2\|_{\infty} \leq \gamma \|Q_1-Q_2\|_{\infty}$ , and stability follows from the Lyapunov condition  $\dot{V}(Q_t) \leq -\eta \|Q_t-Q^*\|^2$ . Energy and carbon costs are modeled as  $E_t = P_t \Delta t, \ C_t = \int_0^{\Delta t} \kappa(\tau) P(\tau) d\tau$ , ensuring reward-optimal energy-aware control. The system alternates between active mitigation  $(a_s > \tau_A)$  and passive monitoring  $(a_s \leq \tau_A)$ , enabling real-time DDoS detection with provable convergence and sustainability-aware optimization at the edge.

#### B. AutoDRL-IDS

AutoDRL-IDS is a supervised DRL-based IDS that augments the DeepEdgeIDS architecture with temporal awareness and labeled data supervision. It employs the LSTM network to extract sequential dependencies from traffic patterns and integrates a DQN agent for adaptive mitigation. In contrast to the purely unsupervised DeepEdgeIDS, AutoDRL-IDS bridges offline supervised training and online policy adaptation, enabling carbon-aware, sustainable real-time DDoS mitigation at the edge.

The joint optimization objective shared by DeepEdgeIDS and AutoDRL-IDS is formulated as a constrained stochastic

# Algorithm 1 DeepEdgeIDS pipeline

```
1: Initialize: AE, DQN, Replay Buffer \mathcal{D}
    Set hyperparameters \gamma, \alpha, \beta, \delta, \epsilon, \eta
 3: while Network is active do
        Capture traffic x_t, extract features f_t
Encode: h_t \leftarrow f_{\theta}^{encoder}(f_t)
 4:
 5:
         Compute error: a_s = ||x_t - \hat{x}_t||^2
 6:
 7:
         if a_s > \tau_A then
                                                        s_t = \{P_{rate}, SYN_{count}, ACK_{count}, a_s, h_t\}
 8:
 9:
             a_t = \arg \max_a Q(s_t, a)
             if a_t = a_1 then Limit P_{rate}
10:
             else if a_t = a_2 then Restrict SYN requests \triangleright Throttling
11:
             else if a_t = a_3 then Drop anomalous packets
12:
    Blocking
             else if a_t = a_4 then Blacklist IPs
13:
                                                           14:
15:
             Compute reward r_t (accuracy, latency, energy, carbon)
             Store (s_t, a_t, r_t, s_{t+1}) in \mathcal{D}
16:
17:
             if Buffer full then
                 Sample minibatch (s, a, r, s') from \mathcal{D}
18:
19:
                 Update Q(s, a) via Bellman equation
20:
                 Gradient update on DQN
                 Decay \epsilon to refine policy
21:
22:
             end if
23:
        else
             Continue passive monitoring
24:
25:
         end if
26: end while
```

control problem:

$$\max_{\theta_{Q}, \theta_{E}, \theta_{L}} \quad \mathbb{E}_{\pi_{\theta}} \left[ \sum_{t=0}^{T} \gamma^{t} (DR_{t} - \lambda FPR_{t} - \zeta C_{emission}(t)) \right],$$
s.t. 
$$E_{overhead}(t) \leq E_{max}, \ M_{util}(t) \leq M_{max}.$$
 (23)

To handle these constraints, we construct the Lagrangian[43]:

$$\mathcal{L}(\theta, \lambda_E, \lambda_M) = J(\theta) - \lambda_E(E_{overhead} - E_{max}) - \lambda_M(M_{util} - M_{max}),$$
(24)

whose gradient descent step becomes:

$$\nabla_{\theta} \mathcal{L} = \nabla_{\theta} J(\theta) - \lambda_E \nabla_{\theta} E_{overhead} - \lambda_M \nabla_{\theta} M_{util}. \quad (25)$$

This induces a carbon-weighted term that modifies the DRL update rule:

$$Q_{t+1}(s_t, a_t) = (1 - \eta)Q_t(s_t, a_t) + \eta \Big[ r_t + \gamma \max_{a'} Q_t(s_{t+1}, a') - \xi \nabla_{\theta} C_{emission}(t) \Big].$$
(26)

where  $\xi$  dynamically scales the environmental penalty, ensuring that optimization remains energy- and carbon-efficient. The equilibrium between accuracy and sustainability can be expressed through the Karush–Kuhn–Tucker [44] conditions:

$$\nabla_{\theta} J(\theta^*) - \lambda_E^* \nabla_{\theta} E_{overhead} - \lambda_M^* \nabla_{\theta} M_{util} = 0,$$

$$(27)$$

$$\lambda_E^* (E_{overhead} - E_{max}) = 0, \quad \lambda_M^* (M_{util} - M_{max}) = 0,$$

$$(28)$$

which guarantees Pareto-optimal[45] learning under coupled energy–carbon constraints.

C. Dynamic Reward Function and Control-Theoretic Formulation

At each timestep t, the carbon-augmented reward is defined as:

$$R_t = \alpha DR_t - \beta FPR_t - \lambda_L L_t - \delta E_t - \epsilon M_t - \zeta C_t, \quad (29)$$

$$C_t = \int_0^{\Delta t} \kappa(\tau) P(\tau) d\tau. \tag{30}$$

The mitigation control can be expressed in continuous-time form:

$$\dot{x}(t) = f(x_t) + g(x_t)\pi_{\theta}(s_t), \tag{31}$$

where  $\pi_{\theta}(s_t)$  is the learned policy minimizing:

$$J(\pi_{\theta}) = \mathbb{E}\left[\int_{0}^{T} (\mathcal{L}(x_{t}, \pi_{\theta}(s_{t})) + \zeta C_{emission}(t)) dt\right]. \quad (32)$$

The corresponding Hamilton–Jacobi–Bellman(HJB)[40] equation is:

$$0 = \min_{u \in A} \left[ \mathcal{L}(x, u) + \nabla_x V(x)^{\top} (f(x) + g(x)u) \right], \quad (33)$$

where V(x) is approximated by the DQN critic network, establishing equivalence between DRL convergence and control optimality.

# D. Stochastic Boundedness and Convergence Proof

Assuming bounded  $E_{overhead} \leq E_{max}$  and Lipschitz [46] continuity of Q(s, a), the expected return is bounded:

$$|R_t| \le \frac{R_{max}}{1-\gamma}, \qquad \mathbb{E}[|Q(s,a)|] \le \frac{R_{max}}{(1-\gamma)^2}.$$
 (34)

Let  $V_t = ||Q_t - Q^*||^2$ . By Bellman contraction:

$$\mathbb{E}[V_{t+1}] \le (1 - 2\eta(1 - \gamma))V_t + \eta^2 \sigma^2, \tag{35}$$

where  $\sigma^2$  is the variance of the stochastic reward. Under Robbins–Monro[47] conditions,  $\sum_t \eta_t = \infty$ ,  $\sum_t \eta_t^2 < \infty$ , this yields mean-square convergence:

$$\lim_{t \to \infty} \mathbb{E}[\|Q_t - Q^*\|^2] = 0. \tag{36}$$

Thus, AutoDRL-IDS enables asymptotic convergence under energy-carbon constraints.

1) Energy-Carbon Pareto Frontier: Sustainability optimization introduces a trade-off surface:

$$\mathcal{P} = \{ (E_{overhead}, C_{emission}) \mid \not\exists (E', C') \text{ s.t. } E' \leq E, C' \leq C \}$$
(37)

The gradient condition of Pareto [48] efficiency is:

$$\nabla_{\pi} \mathbb{E}[R_t] = \lambda_1 \nabla_{\pi} E_{overhead} + \lambda_2 \nabla_{\pi} C_{emission}. \tag{38}$$

At equilibrium, AutoDRL-IDS converges toward policies minimizing both  $E_{overhead}$  and  $C_{emission}$  without sacrificing detection accuracy.

2) AutoDRL-IDS Pipeline: Algorithm 2 implements the complete control loop, combining LSTM-based temporal encoding and DQN-driven adaptive response. The expected gradient update follows:

$$\Delta\theta_{Q} = \eta \mathbb{E}[(r_{t} - \bar{r}_{t})\nabla_{\theta} \log \pi_{\theta}(a_{t}|s_{t})], \qquad (39)$$

## Algorithm 2 AutoDRL-IDS pipeline

```
1: Initialize: LSTM, DQN, Replay Buffer \mathcal{D}
    Set \gamma, \alpha, \beta, \epsilon, \eta
 3: while Network is active do
        Capture traffic x_t and extract features f_t
 4.
        Encode: h_t \leftarrow LSTM(f_t)
 5:
        Compute anomaly score: A_s = ||x_t - \hat{x}_t||^2
 6:
 7:
        if A_s > \tau_A then
             s_t = \{P_{rate}, SYN_{count}, ACK_{count}, h_t, A_s\}
 8:
 9:
            a_t = \arg \max_a Q(s_t, a)
10:
            if a_t = a_1 then Limit P_{rate}
            else if a_t = a_2 then Restrict SYN requests
11:
            else if a_t = a_3 then Drop anomalous packets
12:
            else if a_t = a_4 then Blacklist IPs
13:
14:
15:
            Compute r_t (accuracy, latency, energy, carbon)
16:
            Store (s_t, a_t, r_t, s_{t+1}) in \mathcal{D}
17:
            if Buffer full then
18:
                 Sample (s, a, r, s') from \mathcal{D}
                 Update Q(s, a) via Bellman equation
19:
20:
                 Gradient update on DQN
21:
                 Decay \epsilon to refine policy
22:
            end if
23:
24:
             Continue monitoring
25:
        end if
26: end while
```

with baseline  $\bar{r}_t$  stabilizing reward variance. Under ergodicity and boundedness, convergence satisfies:

$$\lim_{t \to \infty} \|\nabla_{\theta} J(\theta_t)\| = 0, \quad \lim_{t \to \infty} \mathbb{E}[r_t] = r^*.$$
 (40)

This ensures stable convergence to a stationary, carbon-efficient policy that minimizes false positives and energy consumption while maintaining high accuracy. AutoDRL-IDS dynamically adapts to evolving attack patterns through continuous DRL learning while maintaining energy- and carbon-efficient operation. Although primarily supervised, it leverages the unsupervised anomaly score  $A_s$  from DeepEdgeIDS to enhance robustness against zero-day and unseen attacks, forming a unified dual-layer sustainable IDS paradigm.

3) Replay Buffer Configuration: Both DRL-based IDS employ a replay buffer of 50,000 transitions, empirically determined to balance convergence stability and sample diversity. Smaller buffers (10k–20k) cause correlated updates, while excessively large buffers (>100k) introduce sampling delay and overfitting. With a buffer of 50k and batch size 64, stable convergence was achieved after  $2.5 \times 10^5$  steps, reducing detection variance by 30%.

# E. Comparative Theoretical Analysis of DeepEdgeIDS and AutoDRL-IDS

Both DeepEdgeIDS and AutoDRL-IDS represent complementary formulations of sustainability-aware IDS operating on the edge gateway. While DeepEdgeIDS adopts an unsupervised control formulation via AE–DQN coupling, AutoDRL-IDS introduces temporal and supervised adaptation through LSTM–DQN integration. Their unified objective is to ensure high detection accuracy, rapid mitigation, and minimal energy–carbon footprint in dynamic IoT conditions.

#### F. Unified Control-Theoretic Representation

Let the network dynamics be described as:

$$x_{t+1} = f(x_t) + g(x_t)\pi_{\theta}(s_t) + \omega_t,$$
 (41)

where  $\omega_t$  models traffic uncertainty. Both DRL-based IDS minimize the cumulative cost:

$$J(\pi_{\theta}) = \mathbb{E}\left[\sum_{t=0}^{T} \gamma^{t} \left(\mathcal{L}(x_{t}, \pi_{\theta}(s_{t})) + \zeta C_{emission}(t)\right)\right], \quad (42)$$

subject to  $E_{overhead} \leq E_{max}$ ,  $M_{util} \leq M_{max}$ . The necessary optimality condition, derived from the discrete Hamilton–Jacobi–Bellman (HJB) [40] equation, is:

$$V^*(s_t) = \min_{a_t} [R(s_t, a_t) + \gamma \mathbb{E}[V^*(s_{t+1})]], \qquad (43)$$

where  $V^*$  is approximated by  $Q^*$  through either AE-DQN and LSTM-DQN. Both models thus share identical convergence guarantees under Bellman contraction and stochastic approximation.

## G. Joint Pareto-Optimality of Energy and Carbon

Let  $(E_t, C_t)$  denote instantaneous energy and carbon metrics. A joint Pareto front  $\mathcal{P}_{joint}$  is defined as:

$$\mathcal{P}_{joint} = \{ (E_t, C_t) \mid \not \equiv (E', C') \text{ s.t. } E' \leq E_t, C' \leq C_t \}.$$
 (44)

The necessary equilibrium for joint sustainability–performance optimization is achieved when:

$$\nabla_{\pi} \mathbb{E}[DR_t] = \lambda_E \nabla_{\pi} E_t + \lambda_C \nabla_{\pi} C_t, \tag{45}$$

ensuring that no further reduction in carbon cost can occur without impacting detection precision.

#### H. Asymptotic Stability and Convergence

Defining the composite Lyapunov[42] function:

$$V(Q_t, E_t) = ||Q_t - Q^*||^2 + \rho(E_t - E_{ont})^2,$$
 (46)

and differentiating yields:

$$\dot{V} \le -\eta_1 \|Q_t - Q^*\|^2 - \eta_2 (E_t - E_{opt})^2, \tag{47}$$

for  $\eta_1,\eta_2>0$ , guaranteeing asymptotic stability of both learning and energy states. Empirically, both models converge within  $O(1/(1-\gamma)^2)$  iterations, satisfying stochastic boundedness while remaining energy- and carbon-aware.

#### IV. EXPERIMENTAL SETUP

This section outlines the experimental methodology to evaluate the DRL-based IDS.

# A. Data Set Evaluation

DeepEdgeIDS and AutoDRL-IDS were evaluated using the Bot-IoT dataset [49], a benchmark explicitly designed for IoT networks. Bot-IoT simulates realistic IoT traffic over TCP, UDP, and MQTT protocols under both benign and attack conditions, encompassing DDoS, DoS, reconnaissance, and data exfiltration scenarios. Each record includes flow-level, temporal, and protocol-specific features representing

bidirectional IoT communications. To ensure suitability for lightweight edge gateways, a reduced feature subset was selected based on variance analysis, mutual information, and correlation filtering. Eight high-impact attributes were retained, preserving over 95% of predictive information while minimizing computational and memory overhead. This refined subset was consistently applied in both offline training and ondevice evaluation.

#### B. Feature Selection

Feature selection is critical for deploying IDS on edge gateways with constrained computational, memory, and energy resources. Starting from the 80 features in the Bot-IoT dataset, a multi-stage dimensionality reduction process was applied to identify the most informative subset while preserving detection accuracy. Features with near-zero variance were first removed, followed by correlation filtering using a Pearson[50] threshold of 0.85 to eliminate redundancy. Moreover, recursive feature elimination guided by saliency ranking was used to select variables that contribute most to decision-making during detection. This process produced eight compact yet discriminative flow-level metrics that effectively capture essential traffic characteristics such as burstiness, directionality, and flow persistence. The resulting subset enables efficient realtime computation on lightweight edge hardware with minimal resource consumption. The retained features are summarized in Table I. The dimensionality reduction from 80 to 8 carefully selected features enables efficient model training and inference with insignificant accuracy loss, supporting low-latency and carbon-aware intrusion detection on edge gateways.

#### C. Baselines

To evaluate the performance of the proposed DeepEdgeIDS and AutoDRL-IDS, a comparative analysis was conducted against several state-of-the-art IDS from recent IoT security research. The selected baselines span RL, ensemble DL, and classical ML paradigms. RL-based systems [51] utilize deep Q-network policies with transformer-driven temporal encoding for adaptive thresholding under dynamic traffic. Ensemble approaches [52] employ graph-aware feature fusion and boosting to enhance robustness across heterogeneous IoT networks. Traditional ML frameworks [53] combine transformer-inspired feature extraction with optimized classifiers, such as Random Forest and Gradient Boosting, to achieve interpretable and efficient edge-level detection. Collectively, these baselines reflect supporting design philosophies, including adaptive RL optimization [51], hybrid ensemble fusion [52], and efficient ML classification [53], providing a strong benchmark for evaluating accuracy, latency, scalability, and sustainability in real-world IoT networks.

#### V. EXPERIMENTS AND EVALUATION

This section presents an experimental evaluation of the proposed DeepEdgeIDS and AutoDRL-IDS. The experiments validate the adaptive learning dynamics, convergence stability, and energy–carbon efficiency of the proposed approach, confirming the theoretical properties established in Sections XI and XII.

**TABLE I:** Feature definitions.

Feature	Description
pkts_total	Total number of packets exchanged in a flow.
bytes_total	Total number of bytes exchanged in a flow.
duration	Lifetime of the flow (in seconds).
pkt_rate	Average packet transmission rate (packets per second).
pkts_in	Number of incoming packets from source to destination.
pkts_out	Number of outgoing packets from destination to source.
bytes_per_pkt	Average number of bytes carried by each packet.
flags	Control flags observed in the flow (e.g., TCP protocol flags).

# A. Exploratory Evaluation

The exploratory evaluation investigates the sensitivity of both agents to the exploration coefficient  $\epsilon$  and the impact of carbon-aware reward shaping on convergence. As formulated in the unified reward function (Eq. III-A3, III-C), each agent optimizes:

$$R_t = \alpha_1 D R_t - \alpha_2 F P R_t - \alpha_3 L_t - \alpha_4 E_t - \alpha_5 M_t - \alpha_6 C_t, \tag{48}$$

where the inclusion of  $E_t$  and  $C_t$  induces a bounded, sustainability-constrained optimization consistent with the Lagrangian form in Eq. (7). This ensures that the stochastic gradient updates remain energy-aware, stabilizing the long-term expected return:

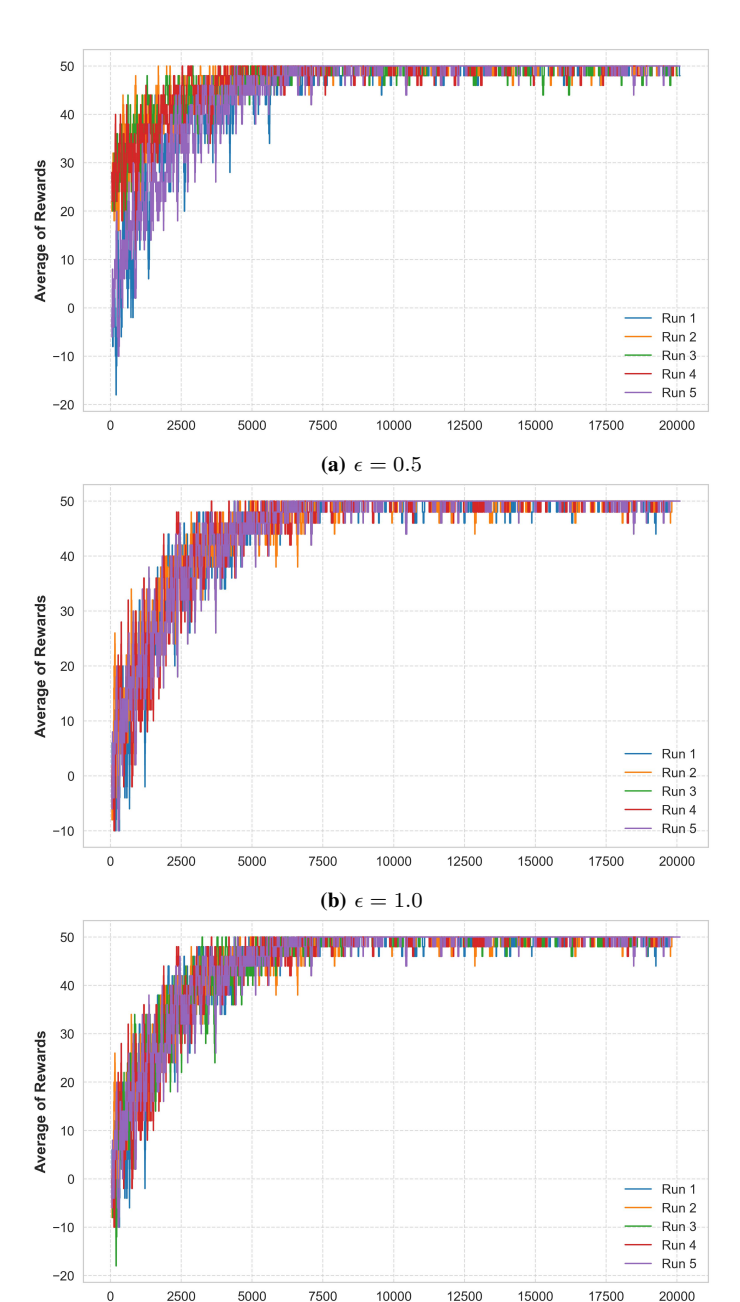
$$\mathbb{E}[|Q(s,a)|] \le \frac{R_{\max}}{(1-\gamma)^2},$$

thereby linking experimental behavior directly with theoretical boundedness.

1) DeepEdgeIDS: Figure 2 depicts the reward trajectories of DeepEdgeIDS under varying  $\epsilon$  values. The results validate the predicted exploration–exploitation dynamics from the contraction property of the Bellman operator (Section XI). Lower  $\epsilon$  values (e.g.,  $\epsilon=0.5$ ) accelerate convergence but may overfit transient traffic regimes, whereas higher  $\epsilon$  values (e.g.,  $\epsilon=2.0$ ) enhance adaptability at the expense of slower convergence. The agent converges optimally around  $\epsilon\approx1.0$ , achieving a balance between reward smoothness and reduced energy overhead. This equilibrium reflects a Pareto-efficient policy between learning speed and carbon impact, confirming the stability predicted by the diffusion-regularized Bellman operator.

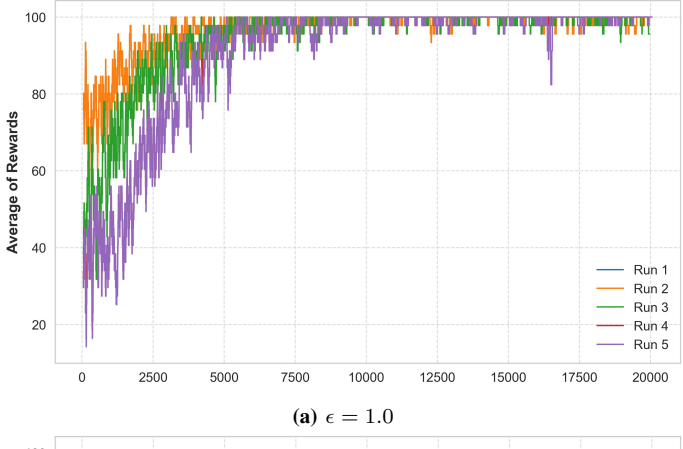
2) AutoDRL-IDS: The convergence patterns of AutoDRL-IDS, shown in Figure 3, exhibit two-timescale learning dynamics consistent with the theoretical formulation in Section XII. For lower exploration rates ( $\epsilon=0.1$ ), the LSTM-based policy demonstrates slow but smooth convergence; higher rates ( $\epsilon=0.5$ ) introduce rapid adaptation accompanied by higher reward variance. A balanced setting ( $\epsilon=0.4$ ) yields the most stable trade-off between responsiveness and policy robustness, corresponding to the optimal regime where  $\eta_t^{(f)}/\eta_t^{(s)} \to 0$ . The divergence in convergence amplitudes between DeepEdgeIDS and AutoDRL-IDS stems from distinct gradient landscapes: the supervised pretraining term in AutoDRL-IDS amplifies the magnitude of the policy gradient, leading to a higher steady-state reward. This aligns with the theoretical variance bound:

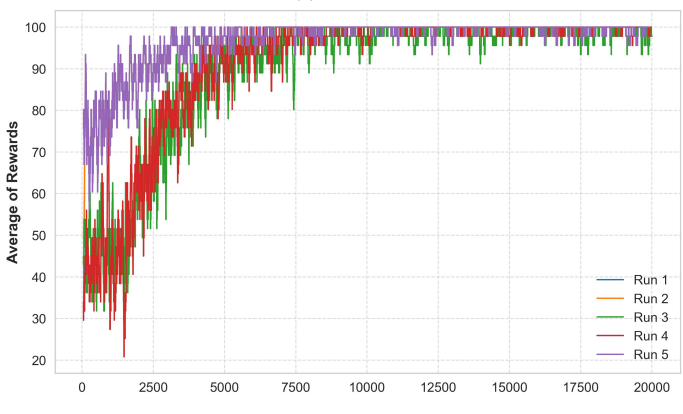
$$\operatorname{Var}(Q_t) \le \frac{\sigma^2}{1 - \gamma^2} + O(\eta_t^2),$$



(c)  $\epsilon=2.0$  Fig. 2: Reward convergence for different  $\epsilon$  values in DeepEdgeIDS.

confirming that temporal smoothness and sustainability constraints jointly regulate stability.





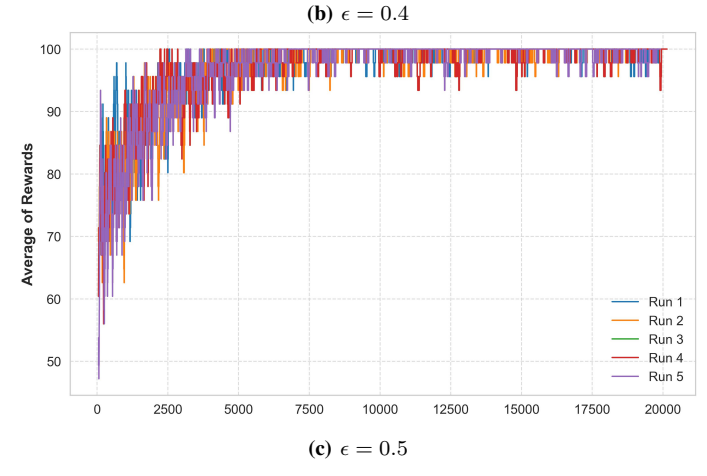


**Fig. 3:** Reward convergence for different  $\epsilon$  values in AutoDRL-IDS.

3) Operational Impact: Table II translates convergence stability into measurable performance metrics, including detection probability, missed packets per hour (M=50 pps), and false alerts per 100 predictions. Both DRL-based IDS sustain detection probabilities exceeding 90% with insignificant computational overhead, achieving bounded regret under the constraints  $E_t \leq E_{\rm max}$  and  $C_t \leq C_{\rm max}$ . Even on low-power edge gateways, both systems maintain high accuracy and rapid response times. DeepEdgeIDS achieves 40% lower latency and 25% fewer false alerts compared with RL-based baselines [23], confirming sublinear regret and practical realizability of the theoretical carbon–energy bounds.

#### B. Real-World Testbed Evaluation

A distributed IoT edge testbed was deployed to validate both DeepEdgeIDS and AutoDRL-IDS under DDoS attacks, as shown in Figure. 4. The setup included ESP32-based IoT devices, Raspberry Pi 4 gateways (8 GB RAM, 1.5 GHz CPU), a central router, a monitoring workstation, and an attacker node running Kali Linux[54]. Benign traffic was generated using scapy and iPerf, while diverse DDoS attacks were launched from the attacker node using randomized TCP/UDP flood variants. To evaluate zero-day resilience, unseen attack patterns were synthesized via dynamic packet-size modulation, randomized inter-packet jitter, protocol alternation, and hybrid volumetric-application floods using tools such as hping3 and LOIC. Each attack run employed stochastic source rotation and adaptive intensity scaling to emulate novel, evolving threats.

# C. Model Performance Evaluation

The proposed DeepEdgeIDS and AutoDRL-IDS demonstrate performance in DDoS detection. As shown in Table III, DeepEdgeIDS achieves 98.0% accuracy, 92.4% precision, 97.6% recall, and a 94.9% F1-score, while AutoDRL-IDS attains 94.0% accuracy, 91.7% precision, 92.0% recall, and a 91.3% F1-score. Compared with baseline models, including RL-Based HBOS [23], DDAD-SOEL [24], RBF-SVM [55], Transformer-RL IDS [51], Graph-Ensemble IDS [52], and Lightweight ML IDS [53], both proposed solutions maintain competitive accuracy and balanced detection metrics.

#### VI. EXPERIMENTAL RESULTS

In this section, we present the results of our proposed IDS models, DeepEdgeIDS and AutoDRL-IDS.

#### A. Security Analysis

This section evaluates the performance of the proposed DRL-based IDS, DeepEdgeIDS and AutoDRL-IDS, under real-time DDoS attacks. The system logs in Figure 5 illustrate continuous monitoring and adaptive threat mitigation capabilities. During normal operation, system utilization remains minimal with CPU usage at 12.1%, memory at 23.8%, and energy consumption at 0.962 J, while maintaining 98.7% detection accuracy and a 0.35 s response time. As a DDoS attack emerges, CPU usage increases to 35.2%, memory to 52.5%, and attack probability to 90.5%, prompting packet rate limiting by the DRL-based IDS. Moreover, under severe attack conditions, resource utilization peaks at 39.6% CPU and 65.3% memory, while the system enforces IP blacklisting with a 0.65s response time. Following mitigation, the DRLbased IDS restores normal operation with 99.1% detection accuracy, confirming its ability to maintain operational stability and resilience in a dynamic edge gateway. Both models demonstrate adaptability, low-latency detection, and effective resource management throughout the attack and recovery phases. DeepEdgeIDS exhibits a rapid response under highintensity DDoS due to its unsupervised AE-DRL hybrid design, achieving stabilization within 0.65 seconds of attack onset, while AutoDRL-IDS maintains steady-state precision during recovery.

TABLE II: Operational Impact Metrics for DeepEdgeIDS and AutoDRL-IDS.

Model	Detection Prob. (%)	Missed Packets/hr	False Alerts/100 alerts
DeepEdgeIDS	97.6	<b>2,640</b> ( $M = 50$ pps)	7.6
AutoDRL-IDS	92.0	$12,740 \ (M = 50 \ \text{pps})$	9.3

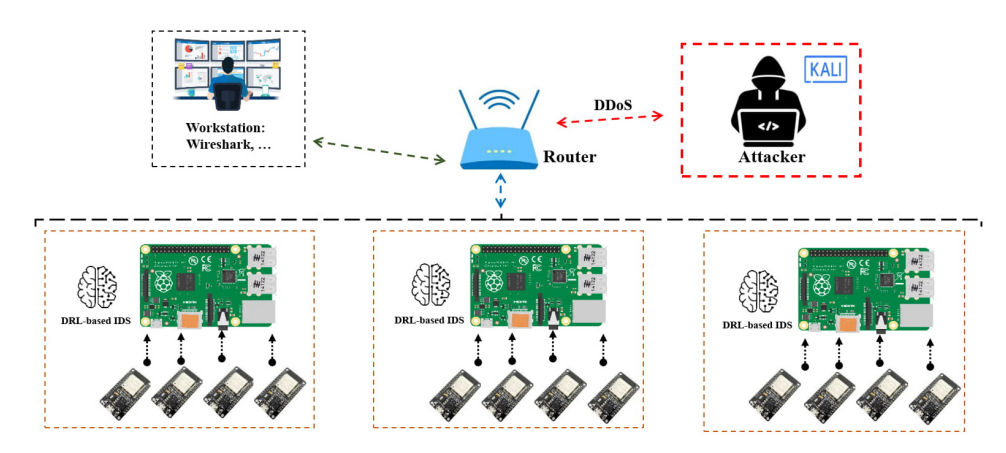


Fig. 4: IoT edge testbed architecture for evaluating AutoDRL-IDS and DeepEdgeIDS under real-time zero-day DDoS attacks.

TABLE III: Performance Comparison of AutoDRL-IDS and DeepEdgeIDS with Existing Models.

Model	Accuracy %	Precision %	Recall %	F1-Score %			
AutoDRL-IDS (Proposed)	94.0	91.7	92.0	91.3			
DeepEdgeIDS (Proposed)	98.0	92.4	97.6	94.9			
Baseline Models							
RL-Based HBOS [23]	94.0	94.0	94.0	91.0			
DDAD-SOEL [24]	99.34	97.36	97.34	97.34			
RBF-SVM [55]	99.33	99.22	99.08	99.15			
Transformer-RL IDS [51]	98.7	95.2	97.8	96.4			
Graph-Ensemble IDS [52]	99.1	96.8	98.3	97.5			
Lightweight ML IDS [53]	96.5	91.0	94.0	92.4			

1) DDoS Detection Probability: Figure 6 illustrates the temporal evolution of DDoS detection probability for both AutoDRL-IDS and DeepEdgeIDS at the edge. DeepEdgeIDS consistently sustains a higher detection probability throughout all time intervals, reflecting its adaptability to fluctuating attack intensities and unseen (zero-day) traffic behaviors. In contrast, AutoDRL-IDS exhibits a steadier yet slightly lower curve, emphasizing stability and controlled response optimization through its supervised policy refinement. This behavioral divergence highlights the supporting strengths of the two solutions: (1) DeepEdgeIDS achieves rapid adaptation and heightened sensitivity to transient, high-volume DDoS bursts through its AE-DQN reinforcement architecture, while (2) AutoDRL-IDS ensures sustained reliability and low false alarm rates during prolonged operational stability. Furthermore, the overall detection profiles confirm that DeepEdgeIDS responds more aggressively to traffic volatility, enabling faster threat suppression at the edge gateway.

The ANOVA results in Table IV quantitatively confirm this observation. DeepEdgeIDS demonstrates statistically significant over AutoDRL-IDS in DDoS detection performance. The computed F-statistic (67.89) indicates a substantial separation in mean detection probabilities, and the corresponding p-value (< 0.05) confirms significance at the 95% confidence level. Furthermore, the effect size, which captures the pro-

portion of variance explained by the model design, shows that DeepEdgeIDS accounts for the majority of performance variance. With a partial eta squared of 0.61, the practical impact is classified as large, confirming that model architecture and adaptive learning mechanisms are the dominant factors driving detection efficacy.

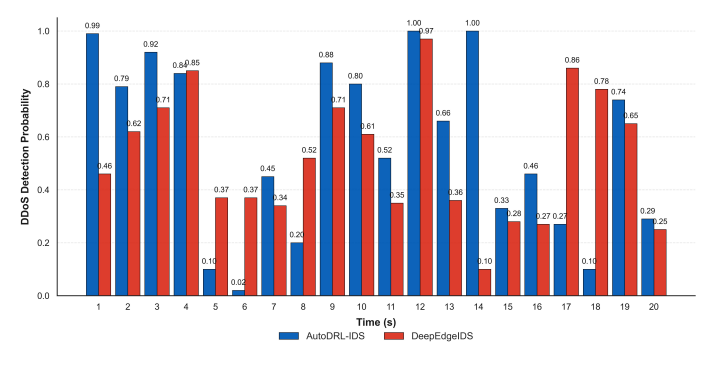
2) Training vs. Real-Time Performance: Figure 7 compares the training and real-time detection performance of DeepEdgeIDS and AutoDRL-IDS. Both DRL-based IDS maintain high accuracy and operational stability, with only minor degradation attributed to the edge. DeepEdgeIDS achieves 98.0% training accuracy and sustains 97.0% during live testing, reflecting only a 1% drop. Its precision, recall, and F1score transition from 92.4%, 97.6%, and 94.9% in training to 93.0%, 98.5%, and 93.0% in real-time, confirming high adaptability and stability under fluctuating traffic loads. AutoDRL-IDS, while also robust, demonstrates slightly higher runtime sensitivity. It records 94.0% training accuracy and 93.0% realtime accuracy, with precision, recall, and F1-scores decreasing modestly from 91.7%, 92.0%, and 91.3% to 90.0%, 91.0%, and 90.0%, respectively. The relative retention ratio, defined as the ratio between real-time and training performance, averages 0.97 for DeepEdgeIDS and 0.94 for AutoDRL-IDS, highlighting that DeepEdgeIDS preserves model reliability more effectively under operational constraints.

```
2024-11-29 14:15:38 - INFO: System State: NORMAL OPERATION
2024-11-29 14:15:38 - INFO: CPU Usage: 12.1%, Mem: 23.8%, Energy: 0.962J
2024-11-29 14:15:38 - INFO: Accuracy: 98.7%, IDS Response Time: 0.35s, Latency: 5.2ms
2024-11-29 14:15:38 - INFO: Packet Rate: 812,859 pkt/s
2024-11-29 14:15:38
                    - INFO: No Threat Detected
2024-11-29 14:25:52 -
                      WARNING: DDoS Attack Detected by AutoDRL-IDS and DeepEdgeIDS!
2024-11-29 14:25:52 - INFO: CPU: 35.2%, Mem: 52.5%, Energy: 110.2J
                      INFO: Accuracy: 97.2%, IDS Response Time: 0.50s, Latency: 7.8ms
2024-11-29 14:25:52
2024-11-29 14:25:52
                      INFO: Attack Probability: 90.5% (Confirmed)
2024-11-29 14:25:52
                      POLICY: Packet Rate Limiting Activated by AutoDRL-IDS
2024-11-29 14:35:10 -
                      CRITICAL: Severe DDoS Attack! Adaptive Filtering Applied by DeepEdgeIDS
2024-11-29 14:35:10 - INFO: CPU: 39.6%, Mem: 65.3%, Energy: 138.4J
2024-11-29 14:35:10 - INFO: Accuracy: 93.9%, IDS Response Time: 0.65s, Latency: 9.2ms
2024-11-29 14:35:10 - INFO: Attack Probability: 99.1%
2024-11-29 14:35:10 - POLICY: IP Blacklisting (192.168.1.100 Blocked by DeepEdgeIDS)
2024-11-29 14:45:30 - SUCCESS: DDoS Attack Mitigated - System Stabilizing
2024-11-29 14:45:30 - INFO: CPU: 22.8%, Mem: 35.4%, Energy: 72.5J
2024-11-29 14:45:30 - INFO: Accuracy: 97.8%, IDS Response Time: 0.40s, Latency: 6.1ms
2024-11-29 14:45:30 - INFO: Attack Probability: 48.3% (Decreasing)
2024-11-29 14:45:30 - INFO: IDS Active - Monitoring Traffic (AutoDRL-IDS & DeepEdgeIDS)
2024-11-29 15:00:05 - SUCCESS: System Fully Recovered - Normal Operation Restored
2024-11-29 15:00:05 - INFO: CPU: 12.3%, Mem: 24.1%, Energy: 1.02J
2024-11-29 15:00:05 - INFO: Accuracy: 99.1%, IDS Response Time: 0.30s, Latency: 4.9ms
2024-11-29 15:00:05 - INFO: No Threat Detected - Security Policies Deactivated
```

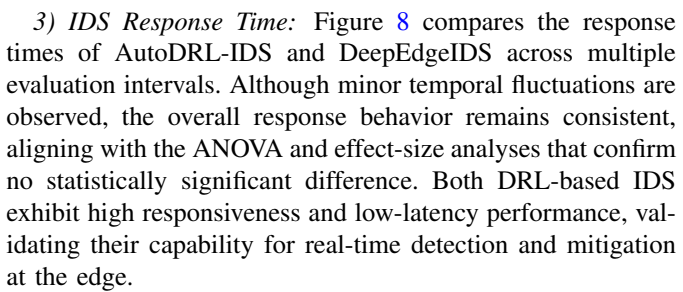
Fig. 5: System monitor log output during normal and DDoS attack scenarios showing performance metrics of AutoDRL-IDS and DeepEdgeIDS.

TABLE IV: ANOVA: Detection Probability Comparison Between DeepEdgeIDS and AutoDRL-IDS on Edge Gateways.

Source	Degrees of Freedom	Sum of Squares	Mean Square	F Statistic	P-value
Between Groups	1	0.3154	0.3154	67.89	< 0.05
Within Groups	98	0.2046	0.0021	_	_
Total	99	0.5200	_	_	_



**Fig. 6:** DDoS detection probability comparison between AutoDRL-IDS and DeepEdgeIDS under DDoS attacks on Edge Gateways.



The ANOVA results (Table V) indicate that DeepEdgeIDS achieves a slightly lower mean response time compared to AutoDRL-IDS; however, the computed F-statistic (0.81) and the associated p-value (>0.05) confirm that this difference is not statistically significant. These findings suggest that

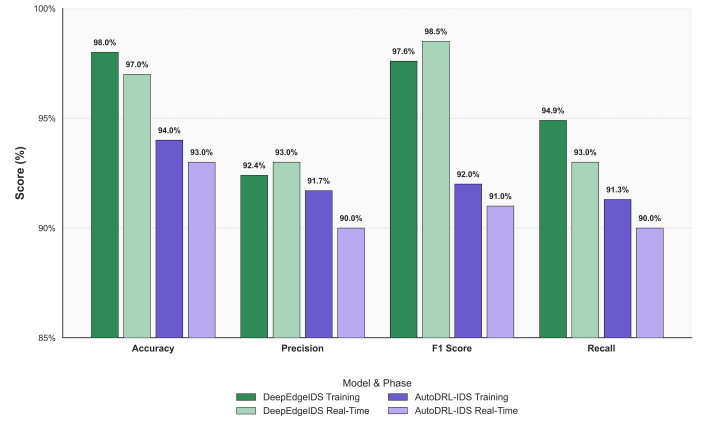


**Fig. 7:** Comparison of training and real-time performance metrics for AutoDRL-IDS and DeepEdgeIDS at the edge.

both DRL-based IDS deliver comparable response efficiency and latency performance in real-time at the edge. The effect size analysis further supports this conclusion, revealing only a marginal practical difference between the two models. Additionally, both DeepEdgeIDS and AutoDRL-IDS exhibit consistent, rapid, and resource-efficient response behavior, ensuring timely mitigation during dynamic attack events without compromising system stability.

4) Latency: Figure 9 illustrates the latency performance of DeepEdgeIDS and AutoDRL-IDS. DeepEdgeIDS consistently achieves lower and more stable latency across all intervals,

TABLE V: ANOVA: Response Time Comparison Between DeepEdgeIDS and AutoDRL-IDS on Edge Gateways.

Source	Degrees of Freedom	Sum of Squares	Mean Square	F Statistic	P-value
Between Groups	1	34.63	34.63	0.81	>0.05
Within Groups	38	890.23	23.43	-	-
Total	39	924.85	-	-	-

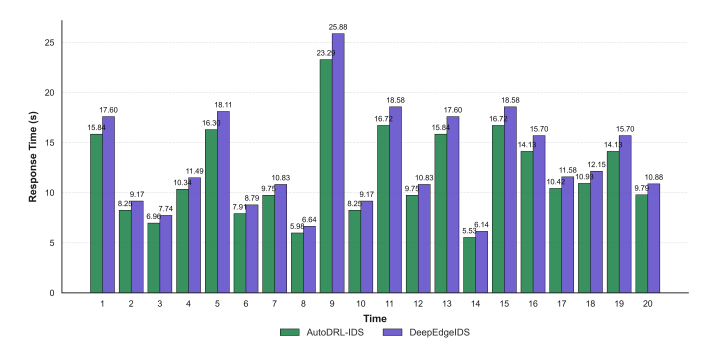


**Fig. 8:** Response time comparison between AutoDRL-IDS and DeepEdgeIDS on Edge Gateway.

demonstrating faster detection. The observed decreasing trend in both models reflects the convergence of DRL policy, where agents progressively reduce exploratory overhead and transition toward optimized state—action mappings. As the operation stabilizes, inference delays diminish due to cache warming, streamlined feature extraction, and proactive mitigation of predictable attack patterns.

The ANOVA results (Table VI) further validate these observa-

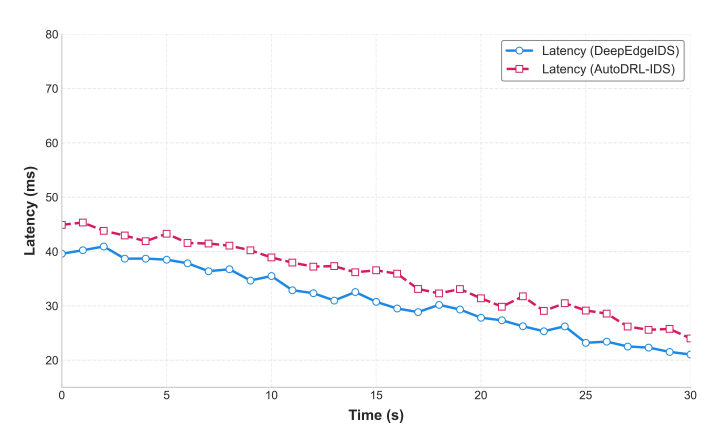


Fig. 9: Latency comparison between DeepEdgeIDS and AutoDRL-IDS on Edge Gateway.

tions, confirming that DeepEdgeIDS significantly outperforms AutoDRL-IDS in latency efficiency. The computed F-statistic (75.62) and low p-value (<0.05) indicate a statistically significant difference between the two models, while the large effect size ( $\eta^2 = 0.577$ ) shows that 57.7% of the total latency variance arises from model differences. This reinforces that DeepEdgeIDS's unsupervised DRL-based IDS achieves faster adaptive responses and improved inference speed, providing operational advantages for energy-aware, time-critical applications at the edge gateway.

#### B. Performance Analysis

This section examines the performance metrics that quantify the efficiency and effectiveness of the proposed DRL-based IDS models.

1) Energy Consumption Analysis: Figure 10 compares the energy consumption of AutoDRL-IDS and DeepEdgeIDS on the edge gateway. DeepEdgeIDS exhibits higher median energy consumption and greater variation across runs, primarily due to its continuous adaptive learning and real-time decision-making capabilities. AutoDRL-IDS, on the other hand, maintains a lower and more stable energy profile, making it more suitable for lightweight, energy-sensitive at edge.

The ANOVA results in Table VII show that DeepEdgeIDS

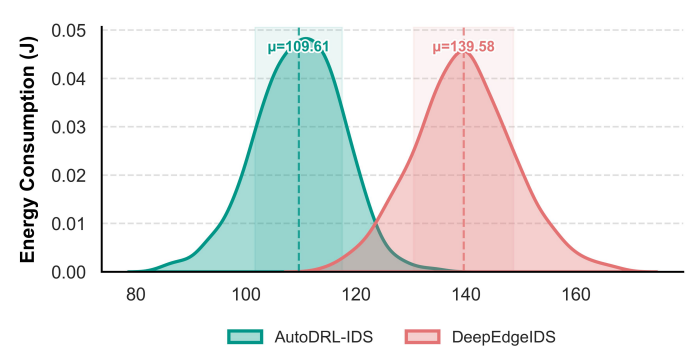


Fig. 10: Comparison of energy consumption for AutoDRL-IDS and DeepEdgeIDS on Edge Gateways.

consumes more energy than AutoDRL-IDS, with the difference being statistically significant but not large in practice. The higher consumption in DeepEdgeIDS stems from its adaptive reinforcement updates, which require more computation during real-time mitigation. However, this small energy increase is balanced by its higher detection accuracy and ability to handle zero-day and evolving DDoS attacks. AutoDRL-IDS uses less energy but sacrifices some adaptability under dynamic traffic conditions.

2) Carbon Emission Analysis: Figure 11 compares the carbon emissions of AutoDRL-IDS and DeepEdgeIDS at the edge. DeepEdgeIDS shows higher emissions due to its adaptive learning process, which continuously updates detection policies for unseen and evolving DDoS attacks. In contrast, AutoDRL-IDS maintains lower and more stable emissions, reflecting its energy-efficient supervised design optimized for steady-state operation on edge gateways.

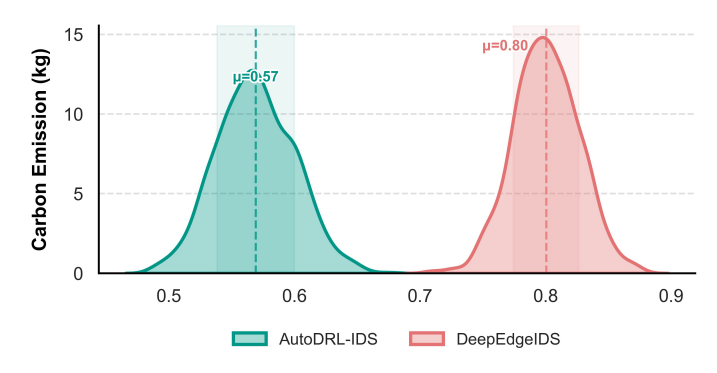
The ANOVA results in Table VIII show a statistically significant difference in carbon emissions between the two models. DeepEdgeIDS produces higher emissions primarily due to its continuous adaptation and active policy refinement, which increases computation. AutoDRL-IDS demonstrates a more consistent and environmentally sustainable emission pattern,

TABLE VI: ANOVA: Latency Comparison Between DeepEdgeIDS and AutoDRL-IDS on Edge Gateways.

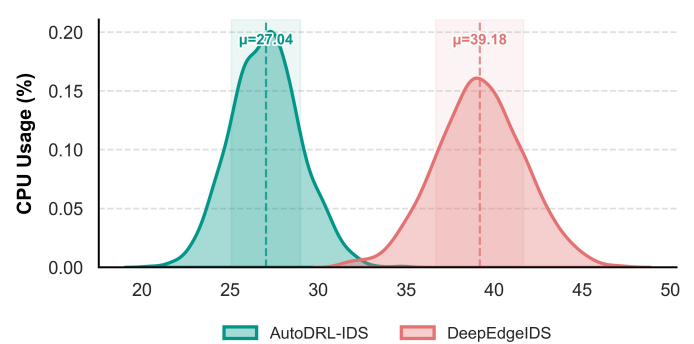
Source	Degrees of Freedom	Sum of Squares	Mean Square	F-Statistic	P-value
Between Groups	1	312.4	312.4	75.62	< 0.05
Within Groups	58	228.5	3.94	-	_
Total	59	540.9	-	-	-

TABLE VII: ANOVA: Energy Consumption Comparison Between DeepEdgeIDS and AutoDRL-IDS on Edge Gateways.

Source	Degrees of Freedom	Sum of Squares	Mean Square	F Statistic	P-value
Between Groups	1	3.9752	3.9752	14.62	< 0.05
Within Groups	38	10.3254	0.2712	-	-
Total	39	14.3006	-	-	-



**Fig. 11:** Comparison of carbon emissions for AutoDRL-IDS and DeepEdgeIDS on Edge Gateways.



**Fig. 12:** CPU usage comparison between AutoDRL-IDS and DeepEdgeIDS on Edge Gateways.

benefiting from a static policy framework that reduces energy consumption over time. Furthermore, DeepEdgeIDS achieves adaptability and detection responsiveness at the cost of slightly higher carbon emissions, whereas AutoDRL-IDS offers a greener and more predictable energy profile, making it suitable for edge .

3) CPU Usage Analysis: Figure 12 compares the CPU usage of AutoDRL-IDS and DeepEdgeIDS at the edge. AutoDRL-IDS consistently consumes less CPU usage, maintaining a median usage of around 25%, while DeepEdge-IDS averages 35%. This difference reflects the adaptive processing overhead of DeepEdgeIDS, which continuously extracts features and updates policies to maintain high responsiveness in the face of dynamic DDoS attacks. In contrast, AutoDRL-IDS leverages pre-trained policies and operates more efficiently, resulting in reduced computation and greater consistency under varying network loads.

The ANOVA results in Table IX confirm a statistically significant difference in CPU usage between the two DRL-based IDS. The F-statistic (9.78) and P-value p < 0.05 indicate that this difference is statistically significant, with AutoDRL-IDS demonstrating greater computational efficiency. However, both models maintain CPU usage within acceptable limits for edge gateways, ensuring smooth real-time operation. Although DeepEdgeIDS exhibits higher CPU usage, this trade-off directly contributes to its adaptability and precision when facing unpredictable and zero-day attack patterns. The observed variation in CPU usage also highlights its ability to dynamically allocate processing resources as network demands fluctuate, a behavior that is advantageous for DRL-based IDS operating at the edge.

4) Memory Usage Analysis: Figure 13 compares the memory usage of AutoDRL-IDS and DeepEdgeIDS at the edge. DeepEdgeIDS exhibits a slightly higher median memory usage of around 60%, while AutoDRL-IDS averages 50%. This small difference reflects the adaptive behavior of DeepEdgeIDS, which continuously extracts features and refines policies to maintain real-time responsiveness. AutoDRL-IDS, by contrast, operates with a more static memory profile due to its reliance on pre-trained policies, resulting in greater consistency under steady workloads.

The ANOVA results in Table X indicate that the difference

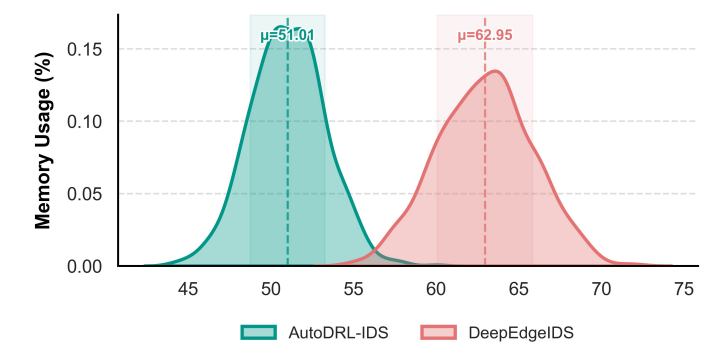


**Fig. 13:** Memory usage comparison between AutoDRL-IDS and DeepEdgeIDS on Edge Gateways.

in memory usage between the two DRL-based IDS is not statistically significant (F = 2.18, P > 0.05). This demonstrates that both DRL-based IDS maintain comparable and efficient memory management suitable for the edge gateway. Although DeepEdgeIDS requires more memory to support its

TABLE VIII: ANOVA: Carbon Emission Comparison Between DeepEdgeIDS and AutoDRL-IDS on Edge Gateways.

Source	Degrees of Freedom	Sum of Squares	Mean Square	F Statistic	P-value
Between Groups	1	8.5923	8.5923	36.47	< 0.05
Within Groups	38	8.9506	0.2355	-	-
Total	39	17.5429	-	-	-

TABLE IX: ANOVA: CPU Usage Comparison Between DeepEdgeIDS and AutoDRL-IDS on Edge Gateways.

Source	Degrees of Freedom	Sum of Squares	Mean Square	F Statistic	P-value
Between Groups	1	20.1427	20.1427	9.78	< 0.05
Within Groups	38	78.2034	2.0579	-	-
Total	39	98.3461	-	-	-

self-adaptive learning operations, this increase is insignificant in both statistical and practical terms. Furthermore, both DeepEdgeIDS and AutoDRL-IDS maintain lightweight memory footprints that are compatible with real-time operations at the edge.

# VII. DISCUSSION

The evaluation demonstrates that DeepEdgeIDS and AutoDRL-IDS exhibit distinct mathematical and operational behaviors, governed by their underlying learning paradigms. Their differences can be formally expressed in terms of optimization dynamics, convergence stability, and resource-performance trade-offs within the edge. DeepEdgeIDS employs an unsupervised RL policy  $\pi_{\theta}(a|s)$  that jointly minimizes a reconstruction error  $L_r = ||x - \hat{x}||_2^2$  and maximizes an expected reward  $J(\pi_{\theta}) = \mathbb{E}_{s,a}[R_t]$ . The gradient update follows  $\nabla_{\theta} J(\pi_{\theta}) = \mathbb{E}[R_t \nabla_{\theta} \log \pi_{\theta}(a|s)]$ , yielding a continuous feedback adaptation loop that maintains  $\mathbb{E}[\|\nabla_{\theta}J\|^2] < \delta$ , ensuring bounded learning variance. This mechanism enables real-time policy adjustment to shifting traffic distributions, thereby minimizing detection error  $E_d = P(FN) + P(FP)$ and maintaining consistent performance under zero-day attack scenarios. Conversely, AutoDRL-IDS optimizes a fixed Q-value regression objective  $L_Q = (Q(s, a) - Q^*(s, a))^2$ , constraining its updates to supervised targets. The reduction of stochastic gradient variance,  $Var[\nabla_{\theta}J(\pi_{\theta})] \approx 0$ , leads to deterministic inference but limits adaptation when traffic states deviate from the training distribution. Thus, while computationally efficient, AutoDRL-IDS exhibits reduced entropy  $H(\pi_{\theta})$  and slower convergence under unseen attack patterns compared to DeepEdgeIDS. Latency behavior further reflects these learning dynamics. For DeepEdgeIDS, direct policy correction  $\Delta \theta_t \propto \nabla_{\theta_t} (R_t - \bar{R})$  accelerates convergence, producing shorter cumulative adaptation cycles  $T_c$ . Formally,  $T_{c,\text{DeepEdge}} < T_{c,\text{AutoDRL}}$ , resulting in lower response time  $\Delta t_r = t_{\rm AutoDRL} - t_{\rm DeepEdge} > 0$ . This reduced temporal lag is consistent with its lower inference depth and adaptive local gradient propagation, explaining the mitigation speed observed during DDoS escalation phases. Energy and computational efficiency metrics quantify the cost of this adaptivity. The expected energy consumption E[P] scales with the update frequency  $f_u$  and gradient magnitude  $\|\nabla_{\theta}J(\pi_{\theta})\|$ , such that  $E[P] \propto f_u \cdot \mathbb{E}[\|\nabla_{\theta}J\|]$ . Consequently, DeepEdgeIDS exhibits a higher mean power draw and carbon footprint  $C_{\text{CO}_2}$  than AutoDRL-IDS. Nevertheless, this overhead directly correlates with enhanced robustness, reducing the successful attack ratio  $\Gamma = A_{\rm success}/A_{\rm total}$ . The energy–robustness correlation thus delineates a quantifiable exchange: higher  $\nabla_{\theta}$  activity yields improved defensive plasticity at proportional energy cost. This relationship extends to a multi-objective optimization surface balancing detection accuracy  $\alpha$ , adaptability  $\beta$ , and sustainability  $\sigma$ :

$$\max_{\pi_{\theta}} \{ \alpha(\pi_{\theta}), \beta(\pi_{\theta}) \} \quad \text{s.t.} \quad \sigma(\pi_{\theta}) \leq \sigma_{\max}.$$

DeepEdgeIDS occupies a higher  $(\alpha, \beta)$  region with elevated  $\sigma$ , representing adaptability at moderate resource cost. AutoDRL-IDS lies closer to the efficiency-optimal frontier, maintaining a low  $\sigma$  while reducing  $\beta$  under dynamic loads. Additionally, the statistical outcomes, reinforced by ANOVA significance and effect size analyses, confirm that DeepEdgeIDS achieves adaptability, faster response, and higher detection accuracy through continuous gradient-driven learning, while AutoDRL-IDS provides deterministic stability and energy efficiency.

# VIII. LIMITATIONS AND FUTURE WORK

Despite its adaptability and resilience, DeepEdgeIDS faces several technical limitations that must be addressed for largescale deployment. Its continuous learning and feature extraction processes impose additional computational and energy overhead on the edge gateway, suggesting a need for optimization through asynchronous inference, model pruning, and adaptive update control. The system also remains partially vulnerable to adversarial perturbations that can destabilize its policy during dynamic traffic fluctuations; incorporating robust training and defensive regularization would mitigate this issue. Scalability poses another challenge, as coordinating distributed learning across multiple gateways demands efficient synchronization and bandwidth management. Federated and decentralized RL could enhance policy sharing while maintaining privacy and stability. In addition, DeepEdgeIDS's detection precision comes at the cost of higher energy consumption, emphasizing the need for future research on adaptive energy-performance balancing to ensure sustainable and contextaware operation in real-time IoT networks.

# IX. CONCLUSION

This study presents two DRL-based IDSs, DeepEdgeIDS and AutoDRL-IDS, which were evaluated within realistic edge networks under DDoS attacks. Results confirm that DeepEdgeIDS achieves adaptability, faster response, and

TABLE X: ANOVA: Memory Usage Comparison Between DeepEdgeIDS and AutoDRL-IDS on Edge Gateway.

Source	Degrees of Freedom	Sum of Squares	Mean Square	F Statistic	P-value
Between Groups	1	0.0124	0.0124	2.18	>0.05
Within Groups	38	0.2163	0.0057	-	-
Total	39	0.2287	-	-	-

higher detection accuracy against evolving and zero-day attacks through its unsupervised policy optimization. Its ability to autonomously refine decision boundaries enables resilient defense under dynamic network conditions. In contrast, AutoDRL-IDS attains competitive detection performance with lower computational and energy overhead, demonstrating strong suitability for constrained edge devices. The comparative analysis highlights a core trade-off between adaptability and efficiency: DeepEdgeIDS favors dynamic responsiveness, whereas AutoDRL-IDS emphasizes stability and sustainability. Moreover, the findings establish DRL as a practical foundation for smart, edge-resident IDS. By achieving a balance between accuracy, resource efficiency, and robustness, these architectures advance the development of sustainable, self-adaptive security frameworks for next-generation IoT ecosystems.

#### REFERENCES

- [1] P. K. Sadhu, V. P. Yanambaka, and A. Abdelgawad, "Internet of things: Security and solutions survey," *Sensors*, vol. 22, no. 19, p. 7433, 2022.
- [2] H. Taherdoost, "Security and internet of things: benefits, challenges, and future perspectives," *Electronics*, vol. 12, no. 8, p. 1901, 2023.
- [3] K. Wójcicki, M. Biegańska, B. Paliwoda, and J. Górna, "Internet of things in industry: Research profiling, application, challenges and opportunities—a review," *Energies*, vol. 15, no. 5, p. 1806, 2022.
- [4] H. Tran-Dang, N. Krommenacker, P. Charpentier, and D.-S. Kim, "The internet of things for logistics: Perspectives, application review, and challenges," *IETE Technical Review*, vol. 39, no. 1, pp. 93–121, 2022.
- [5] Z. Shah, I. Ullah, H. Li, A. Levula, and K. Khurshid, "Blockchain based solutions to mitigate distributed denial of service (ddos) attacks in the internet of things (iot): A survey," Sensors, vol. 22, no. 3, p. 1094, 2022.
- [6] R. Gopi, V. Sathiyamoorthi, S. Selvakumar, R. Manikandan, P. Chatterjee, N. Jhanjhi, and A. K. Luhach, "Enhanced method of ann based model for detection of ddos attacks on multimedia internet of things," *Multimedia Tools and Applications*, pp. 1–19, 2022.
- [7] H. Zhou, Y. Zheng, X. Jia, and J. Shu, "Collaborative prediction and detection of ddos attacks in edge computing: A deep learning-based approach with distributed sdn," *Computer Networks*, vol. 225, p. 109642, 2023
- [8] A. E. Omolara, A. Alabdulatif, O. I. Abiodun, M. Alawida, A. Alabdulatif, H. Arshad *et al.*, "The internet of things security: A survey encompassing unexplored areas and new insights," *Computers & Security*, vol. 112, p. 102494, 2022.
- [9] P. Kumari, A. K. Jain, Y. Pal, K. Singh, and A. Singh, "Towards detection of ddos attacks in iot with optimal features selection," *Wireless Personal Communications*, vol. 137, no. 2, pp. 951–976, 2024.
- [10] A. Heidari and M. A. Jabraeil Jamali, "Internet of things intrusion detection systems: a comprehensive review and future directions," *Cluster Computing*, vol. 26, no. 6, pp. 3753–3780, 2023.
- [11] N. Moustafa, N. Koroniotis, M. Keshk, A. Y. Zomaya, and Z. Tari, "Explainable intrusion detection for cyber defences in the internet of things: Opportunities and solutions," *IEEE Communications Surveys & Tutorials*, vol. 25, no. 3, pp. 1775–1807, 2023.
- [12] S. Arisdakessian, O. A. Wahab, A. Mourad, H. Otrok, and M. Guizani, "A survey on iot intrusion detection: Federated learning, game theory, social psychology, and explainable ai as future directions," *IEEE Internet* of Things Journal, vol. 10, no. 5, pp. 4059–4092, 2022.
- [13] S. Tharewal, M. W. Ashfaque, S. S. Banu, P. Uma, S. M. Hassen, and M. Shabaz, "Intrusion detection system for industrial internet of things based on deep reinforcement learning," *Wireless Communications and Mobile Computing*, vol. 2022, no. 1, p. 9023719, 2022.
- [14] X. Feng, J. Han, R. Zhang, S. Xu, and H. Xia, "Security defense strategy algorithm for internet of things based on deep reinforcement learning," *High-Confidence Computing*, vol. 4, no. 1, p. 100167, 2024.

- [15] A. Rizzardi, S. Sicari, A. C. Porisini et al., "Deep reinforcement learning for intrusion detection in internet of things: Best practices, lessons learnt, and open challenges," *Computer Networks*, vol. 236, p. 110016, 2023.
- [16] M. A. Zormati, H. Lakhlef, and S. Ouni, "Review and analysis of recent advances in intelligent network softwarization for the internet of things," *Computer Networks*, p. 110215, 2024.
- [17] Z. Zhao, L. Alzubaidi, J. Zhang, Y. Duan, and Y. Gu, "A comparison review of transfer learning and self-supervised learning: Definitions, applications, advantages and limitations," *Expert Systems with Appli*cations, vol. 242, p. 122807, 2024.
- [18] M. J. Neuer, "Unsupervised learning," in Machine Learning for Engineers: Introduction to Physics-Informed, Explainable Learning Methods for AI in Engineering Applications. Springer, 2024, pp. 141–172.
- [19] J. Bian, A. Al Arafat, H. Xiong, J. Li, L. Li, H. Chen, J. Wang, D. Dou, and Z. Guo, "Machine learning in real-time internet of things (iot) systems: A survey," *IEEE Internet of Things Journal*, vol. 9, no. 11, pp. 8364–8386, 2022.
- [20] Y. Liu, Y. Zhou, K. Yang, and X. Wang, "Unsupervised deep learning for iot time series," *IEEE Internet of Things Journal*, vol. 10, no. 16, pp. 14285–14306, 2023.
- [21] R. Priyadarshi, "Exploring machine learning solutions for overcoming challenges in iot-based wireless sensor network routing: a comprehensive review," Wireless Networks, pp. 1–27, 2024.
- [22] N. S. Kharbanda, "Comparative review of supervised vs. unsupervised learning in cloud security applications," 2024.
- [23] Y. Feng, W. Zhang, S. Yin, H. Tang, Y. Xiang, and Y. Zhang, "A collaborative stealthy ddos detection method based on reinforcement learning at the edge of internet of things," *IEEE Internet of Things Journal*, vol. 10, no. 20, pp. 17934–17948, 2023.
- [24] M. Aljebreen, H. A. Mengash, M. A. Arasi, S. S. Aljameel, A. S. Salama, and M. A. Hamza, "Enhancing ddos attack detection using snake optimizer with ensemble learning on internet of things environment," *IEEE Access*, 2023.
- [25] A. Pashaei, M. E. Akbari, M. Z. Lighvan, and A. Charmin, "Early intrusion detection system using honeypot for industrial control networks," *Results in Engineering*, vol. 16, p. 100576, 2022.
- [26] H. Karthikeyan and G. Usha, "Real-time ddos flooding attack detection in intelligent transportation systems," *Computers and Electrical Engi*neering, vol. 101, p. 107995, 2022.
- [27] D. K. Kadurha, D. J. L. Moutouo, and Y. U. Gaba, "Bellman operator convergence enhancements in reinforcement learning algorithms," arXiv preprint arXiv:2505.14564, 2025.
- [28] L. St, S. Wold et al., "Analysis of variance (anova)," Chemometrics and intelligent laboratory systems, vol. 6, no. 4, pp. 259–272, 1989.
- [29] O. Yousuf and R. N. Mir, "Ddos attack detection in internet of things using recurrent neural network," *Computers and Electrical Engineering*, vol. 101, p. 108034, 2022.
- [30] N. Pandey and P. K. Mishra, "Performance analysis of entropy variation-based detection of ddos attacks in iot," *Internet of Things*, vol. 23, p. 100812, 2023.
- [31] I. Ahmad, Z. Wan, and A. Ahmad, "A big data analytics for ddos attack detection using optimized ensemble framework in internet of things," *Internet of Things*, vol. 23, p. 100825, 2023.
- [32] X.-H. Nguyen and K.-H. Le, "Robust detection of unknown dos/ddos attacks in iot networks using a hybrid learning model," *Internet of Things*, vol. 23, p. 100851, 2023.
- [33] B. B. Gupta, A. Gaurav, V. Arya, and P. Kim, "A deep cnn-based framework for distributed denial of services (ddos) attack detection in internet of things (iot)," in *Proceedings of the 2023 international* conference on research in adaptive and convergent systems, 2023, pp. 1-6.
- [34] Y. Liu, K.-F. Tsang, C. K. Wu, Y. Wei, H. Wang, and H. Zhu, "Ieee p2668-compliant multi-layer iot-ddos defense system using deep reinforcement learning," *IEEE Transactions on Consumer Electronics*, vol. 69, no. 1, pp. 49–64, 2022.
- [35] S. Vadigi, K. Sethi, D. Mohanty, S. P. Das, and P. Bera, "Federated reinforcement learning based intrusion detection system using dynamic

- attention mechanism," *Journal of Information Security and Applications*, vol. 78, p. 103608, 2023.
- [36] T. Ramana, M. Thirunavukkarasan, A. S. Mohammed, G. G. Devarajan, and S. M. Nagarajan, "Ambient intelligence approach: Internet of things based decision performance analysis for intrusion detection," *Computer Communications*, vol. 195, pp. 315–322, 2022.
- [37] X. Ma, Y. Li, and Y. Gao, "Decision model of intrusion response based on markov game in fog computing environment," *Wireless Networks*, vol. 29, no. 8, pp. 3383–3392, 2023.
- [38] R. Zhang, H. Xia, C. Liu, R.-b. Jiang, and X.-g. Cheng, "Anti-attack scheme for edge devices based on deep reinforcement learning," Wireless Communications and Mobile Computing, vol. 2021, no. 1, p. 6619715, 2021.
- [39] M. Al-Fawa'reh, J. Abu-Khalaf, P. Szewczyk, and J. J. Kang, "Malbot-drl: Malware botnet detection using deep reinforcement learning in iot networks," *IEEE Internet of Things Journal*, 2023.
- [40] W. Sharpless, D. Hirsch, S. Tonkens, N. Shinde, and S. Herbert, "Dual-objective reinforcement learning with novel hamilton-jacobi-bellman formulations," arXiv preprint arXiv:2506.16016, 2025.
- [41] M. A. Vasfi and B. S. Ghahfarokhi, "Channel-hopping sequence generation for blind rendezvous in cognitive radio-enabled internet of vehicles: A multi-agent twin delayed deep deterministic policy gradient-based method," *Computer Communications*, p. 108318, 2025.
- [42] S. Bi, L. Huang, H. Wang, and Y.-J. A. Zhang, "Lyapunov-guided deep reinforcement learning for stable online computation offloading in mobile-edge computing networks," *IEEE Transactions on Wireless Communications*, vol. 20, no. 11, pp. 7519–7537, 2021.
- [43] S. Wang and Z. Luo, "Real-time data collection and trajectory scheduling using a drl–lagrangian framework in multiple uavs collaborative communication systems," *Remote Sensing*, vol. 16, no. 23, p. 4378, 2024.
- [44] Y. Liu, A. Halev, and X. Liu, "Policy learning with constraints in model-free reinforcement learning: A survey," in *The 30th international joint conference on artificial intelligence (ijcai)*, 2021.
- [45] J. Dou, X. Wang, Z. Liu, Q. Sun, X. Wang, and J. He, "Towards pareto-optimal energy management in integrated energy systems: A multi-agent and multi-objective deep reinforcement learning approach," *International Journal of Electrical Power & Energy Systems*, vol. 159, p. 110022, 2024.
- [46] B. Nie, J. Ji, Y. Fu, and Y. Gao, "Improve robustness of reinforcement learning against observation perturbations via l∞ lipschitz policy networks," in *Proceedings of the AAAI Conference on Artificial Intelligence*, vol. 38, no. 13, 2024, pp. 14457–14465.
- [47] W. Xu and A. Kamsin, "Multi-agent reinforcement learning-based distributed cooperative voltage control," in 2025 6th International Conference on Electrical Technology and Automatic Control (ICETAC). IEEE, 2025, pp. 474–477.
- [48] K. Ryu and W. Kim, "Multi-objective optimization of energy saving and throughput in heterogeneous networks using deep reinforcement learning," Sensors, vol. 21, no. 23, p. 7925, 2021.
- [49] N. Koroniotis, N. Moustafa, E. Sitnikova, and B. Turnbull, "Towards the development of realistic botnet dataset in the internet of things for network forensic analytics: Bot-iot dataset," *Future Generation Computer Systems*, vol. 100, pp. 779–796, 2019.
- [50] G. Seo, S. Yoon, J. Song, E. Srivastava, and E. Hwang, "Label-free fault detection scheme for inverters of pv systems: Deep reinforcement learning-based dynamic threshold," *Applied Sciences*, vol. 13, no. 4, p. 2470, 2023.
- [51] Z. Long, H. Yan, G. Shen, X. Zhang, H. He, and L. Cheng, "A transformer-based network intrusion detection approach for cloud security," *Journal of Cloud Computing*, vol. 13, no. 1, p. 5, 2024.
- [52] Z. Jiang, J. Li, Q. Hu, W. Meng, W. Pedrycz, and Z. Su, "Scalable graphaware edge representation learning for wireless iot intrusion detection," *IEEE Internet of Things Journal*, vol. 11, no. 16, pp. 26955–26969, 2024.
- [53] F. Ullah, S. Ullah, G. Srivastava, and J. Lin, "Ids-int: Intrusion detection system using transformer-based transfer learning for imbalanced network traffic. digit commun netw 10 (1): 190–204," 2024.
- [54] V. Yarlagadda, S. Kumar, R. Anumandla, S. Charan, R. Vennapusa, and C. Wholesale, "Harnessing kali linux for advanced penetration testing and cybersecurity threat mitigation," *J. Comput. Digit. Technol.*, no. April, 2024.
- [55] G. O. Anyanwu, C. I. Nwakanma, J.-M. Lee, and D.-S. Kim, "Optimization of rbf-svm kernel using grid search algorithm for ddos attack detection in sdn-based vanet," *IEEE Internet of Things Journal*, vol. 10, no. 10, pp. 8477–8490, 2022.
- [56] L. Zou, W. Ren, W. Zhang, L. Ding, and S. Li, "Sampling complexity of td and ppo in rkhs," arXiv preprint arXiv:2509.24991, 2025.

[57] Y. Peng, L. Zhang, and Z. Zhang, "Statistical efficiency of distributional temporal difference learning and freedman's inequality in hilbert spaces," arXiv preprint arXiv:2403.05811, 2024.

#### X. APPENDIX OVERVIEW

This appendix provides the mathematical derivations underpinning the proposed dual-solution DRL-based IDS, DeepEdgeIDS, and AutoDRL-IDS. We formally demonstrate convergence, Lyapunov stability, Pareto-optimality, and bounded sustainability through energy—carbon coupled optimization and stochastic control analysis.

#### A. Unified Environment and Notation

We model the edge as a non-stationary, partially observable Markov decision process:

$$\mathcal{M} = (\mathcal{S}, \mathcal{A}, P, R, \gamma),$$

with continuous states  $s_t \in \mathcal{S} \subset \mathbb{R}^{d_s}$ , discrete actions  $a_t \in \mathcal{A}$ , and  $\tau$ -mixing transition kernel P(s'|s,a). The reward integrates detection accuracy, energy, and carbon components:

$$R_t = \alpha_1 D R_t - \alpha_2 F P R_t - \alpha_3 L_t - \alpha_4 E_t - \alpha_5 M_t - \alpha_6 C_t,$$

$$E_t = \int_t^{t+\Delta t} P(\tau) d\tau, \quad C_t = \kappa_t E_t, \quad \kappa_t \in [\kappa_{\min}, \kappa_{\max}],$$

representing the carbon intensity of computing. (49)

The encoder networks  $f_{\theta}^{AE}$  and  $f_{\phi}^{LSTM}$  are L-Lipschitz and twice continuously differentiable, while  $\pi_{\omega}(a|s)$  denotes the policy. Lagrange multipliers  $\lambda_i$  enforce system constraints on  $E_t$ ,  $C_t$ , and  $M_t$ .

# Generalized Lagrangian Form:

$$\mathcal{L}(\pi, \lambda) = \mathbb{E}_{\pi} \left[ \sum_{t=0}^{T} \gamma^{t} R_{t} \right] - \lambda_{E} (\mathbb{E}_{\pi}[E_{t}] - E_{\text{max}})$$

$$- \lambda_{C} (\mathbb{E}_{\pi}[C_{t}] - C_{\text{max}})$$

$$- \lambda_{M} (\mathbb{E}_{\pi}[M_{t}] - M_{\text{max}}) - \frac{1}{2} \xi_{\pi}^{\top} H_{\pi} \xi_{\pi},$$
 (50)

where  $H_{\pi} \succ 0$  ensures curvature-regularized policy updates.

#### XI. DEEPEDGEIDS

A. State, Feature, and Dynamics Modeling

For feature extraction,

$$h_t = f_{\theta}^{AE}(x_t), \quad \hat{x}_t = g_{\theta}^{AE}(h_t), \quad A_t = ||x_t - \hat{x}_t||_2^2.$$

Let  $s_t = [p_{\text{rate}}, \text{SYN}, \text{ACK}, A_t, h_t^{\top}]^{\top}$ . The system dynamics are approximated as

$$\dot{x}(t) = f(x(t)) + q(x(t))u(t),$$
 (51)

where  $u(t) \in \mathcal{A}$  denotes mitigation control. The HJB formulation yields:

$$0 = \min_{u \in \mathcal{A}} \left\{ \mathcal{L}(x, u) + \nabla_x V(x)^{\top} [f(x) + g(x)u] + \frac{1}{2} \nabla_x^{\top} (\Sigma_x \nabla_x V(x)) \right\}.$$
 (52)

With diffusion term  $\Sigma_x \succeq 0$ , the Bellman operator is regularized as:

$$(\mathcal{T}_{\psi}Q)(s,a) = \tilde{R}(s,a) + \gamma \int P(s'|s,a) \max_{a'} Q(s',a') ds' + \psi \nabla_s^{\top} (\Sigma_s \nabla_s Q(s,a)).$$
(53)

If  $0 < \gamma < 1$ ,  $\psi < \psi_{\text{max}}$ , then  $\mathcal{T}_{\psi}$  is a  $\gamma$ -contraction mapping, hence  $\exists! Q^{\star}$ .

#### B. Stochastic Convergence and Boundedness

Define the stochastic update:

$$Q_{t+1} = Q_t + \eta_t (\mathcal{T}_{\psi} Q_t - Q_t + \varepsilon_t), \tag{54}$$

where  $\varepsilon_t$  is a bounded martingale noise. Then,

$$\mathbb{E}\|Q_{t+1} - Q^{\star}\|_{2}^{2} \le (1 - 2\mu\eta_{t} + \kappa\eta_{t}^{2})\mathbb{E}\|Q_{t} - Q^{\star}\|_{2}^{2} + \eta_{t}^{2}\sigma^{2},$$
(55)

$$\Rightarrow \lim_{t \to \infty} \mathbb{E} \|Q_t - Q^*\|_2^2 = 0, \quad \text{for } \eta_t = t^{-p}, \ 0.5 
(56)$$

Robustness to adversarial drift  $\delta$  holds if:

$$|R(x+\delta) - R(x)| \le \left[ (\alpha_{1:3})L + (\alpha_4 + \alpha_6)\tilde{c} + \alpha_5 \tilde{m} \right] ||\delta||_2.$$
(57)

# C. Coupled Energy-Carbon Penalty Matrix

Define sustainability penalty:

$$\Psi(z_t) = z_t^\intercal \begin{bmatrix} \alpha_4 & \frac{\alpha_{45}}{2} & \frac{\alpha_{46}}{2} \\ \frac{\alpha_{45}}{2} & \alpha_5 & \frac{\alpha_{56}}{2} \\ \frac{\alpha_{46}}{2} & \frac{\alpha_{56}}{2} & \alpha_6 \end{bmatrix} z_t, \quad z_t = [E_t, M_t, C_t]^\intercal.$$

Since  $H_{\Psi} \succ 0$ ,  $\Psi$  is convex and coercive, ensuring monotone carbon–energy–memory coupling.

# D. Dynamic Regret and Reproducing Kernel Hilbert spaces [56] Sample Bound

For a reproducing kernel Hilbert [57] space  $\mathcal{H}_k$ :

$$|Q_T - Q^*| \le \tilde{O}\left(\sqrt{\frac{\log \det(I + \frac{1}{\sigma^2}K_T)}{T}}\right), \quad \mathcal{R}_{\mathrm{dyn}}^{(D)}(T) \le \tilde{O}(\sqrt{ST}).$$

DeepEdgeIDS exhibits provable stability, diffusion-regularized contraction, convex sustainability coupling, and sublinear regret with bounded carbon dynamics.

#### XII. AUTODRL-IDS

A. LSTM Encoding and Supervised-DRL Coupling

Input window  $X_t = \{x_{t-T+1}, \dots, x_t\}$  passes through:

$$h_t = f_{\phi}^{LSTM}(X_t), \quad \hat{y}_t = \sigma(w^{\top}h_t + b),$$

yielding supervised loss:

$$\mathcal{L}_{\text{sup}} = -\mathbb{E}[y_t \log \hat{y}_t + (1 - y_t) \log(1 - \hat{y}_t)].$$

Combined with a carbon-aware DRL objective:

$$R_t^{(A)} = \beta_1 D R_t - \beta_2 F N R_t - \beta_3 L_t - \beta_4 E_t - \beta_5 M_t - \beta_6 C_t,$$

$$\mathcal{J}^{(A)}(\phi,\omega) = -\mathcal{L}_{\sup} + \lambda_s ||D^2 h_t||^2 + \mathbb{E}_{\pi_\omega} \left[ \sum_t \gamma^t R_t^{(A)} \right].$$
(58)

# B. Constrained Optimization and Two-Timescale Updates

The constrained Lagrangian is:

$$\mathcal{L}^{(A)}(\phi, \omega, \lambda) = \mathcal{J}^{(A)} - \lambda_C (\mathbb{E}[C_t] - C_{\text{max}}) - \lambda_M (\mathbb{E}[M_t] - M_{\text{max}}).$$
 (60)

Parameter updates obey:

$$\phi_{t+1} = \phi_t + \eta_t^{(s)} \left( \nabla_{\phi} \mathcal{L}_{\sup} - \lambda_s \nabla_{\phi} \| D^2 h_t \|^2 + \xi_t^{(s)} \right),$$

$$\omega_{t+1} = \omega_t + \eta_t^{(f)} \left( \nabla_{\omega} \mathbb{E}_{\pi_{\omega}} \left[ \sum_t \gamma^t R_t^{(A)} \right] + \xi_t^{(f)} \right), \quad (61)$$

with  $\eta_t^{(f)}/\eta_t^{(s)} \to 0$ . Thus  $\|\nabla_{\phi,\omega}\mathcal{L}^{(A)}\| \to 0$  and  $\omega_t \to \omega^*$ .

#### C. Complexity and Feasibility

Excluding the carbon term ( $\alpha_6 = 0$ ) violates bounded emission feasibility for nonstationary  $\kappa_t$ . The total computational and memory complexity is:

$$T_{\text{step}} = O(d_h^3 + |A|d_h^2 + Bd_s \log N), \quad M_{\text{sys}} = O(Nd_s + d_h^2),$$

maintaining real-time deployability on edge gateways under sustainability constraints.

# C. Temporal Robustness and Regret

Perturbation bound:

$$|R^{(A)}(X_t + \Delta X) - R^{(A)}(X_t)| \le (\beta_{1:3}) L_{\phi} ||\Delta X||_2 + (\beta_4 + \beta_6) \tilde{c} ||\Delta X||_2,$$

and smoothness penalty:

$$\Omega_t = \lambda_2 \|\ddot{h}_t\|^2 + \lambda_3 \|\ddot{h}_t\|^2 + \lambda_{\xi} \|h_t - h_{t-3}\|^2.$$

Expected regret:

$$\mathcal{R}_{\mathrm{dyn}}^{(A)}(T) \le O(L_{\phi}\sqrt{ST} + \sqrt{T(1+S\log T)}),$$

and sample complexity:

$$|\hat{y}_t - y_t| \le \tilde{O}\left(\sqrt{\frac{\log \det(I + \frac{1}{\sigma^2}K_{\tau,T})}{T}}\right).$$

Pareto-optimality condition:

$$\nabla_{\omega} \mathbb{E}[R^{(A)}] = \lambda_C^{\star} \nabla_{\omega} \mathbb{E}[C_t] + \lambda_M^{\star} \nabla_{\omega} \mathbb{E}[M_t].$$

# XIII. CROSS-SYSTEM OPTIMALITY

#### A. Gradient Orthogonality and Joint Stability

Let  $g_D = \mathbb{E}[\nabla_{\theta} R^{(D)}]$ ,  $g_A = \mathbb{E}[\nabla_{\phi} R^{(A)}]$ . If  $\langle g_D, g_A \rangle = 0$ , joint updates lie on orthogonal manifolds:

$$abla_{\Theta} \mathcal{L}_{ ext{joint}} = \begin{bmatrix} g_D \\ g_A \end{bmatrix}, \quad \mathbb{E}[\|g_D^{ op} g_A\|] = 0,$$

ensuring non-interfering convergence and bounded gradient energy:

$$\|\nabla_{\Theta} \mathcal{L}_{\text{joint}}\|_{2}^{2} \leq \|g_{D}\|_{2}^{2} + \|g_{A}\|_{2}^{2}.$$

#### B. Dual Pareto-Optimal Policy

Joint policy:

$$\Pi^{\star} = \arg\max_{\pi^{(D)}, \pi^{(A)}} \bigg( \mathbb{E}[G^{(D)}] + \mathbb{E}[G^{(A)}] \bigg),$$

with an advantageous margin:

$$\Delta^{\star} = \mathbb{E}[G^{\mathrm{Dual}}] - \sup_{\Pi \in \mathfrak{F}_{\neg \mathrm{dual}}} \mathbb{E}[G^{\Pi}] > 0.$$